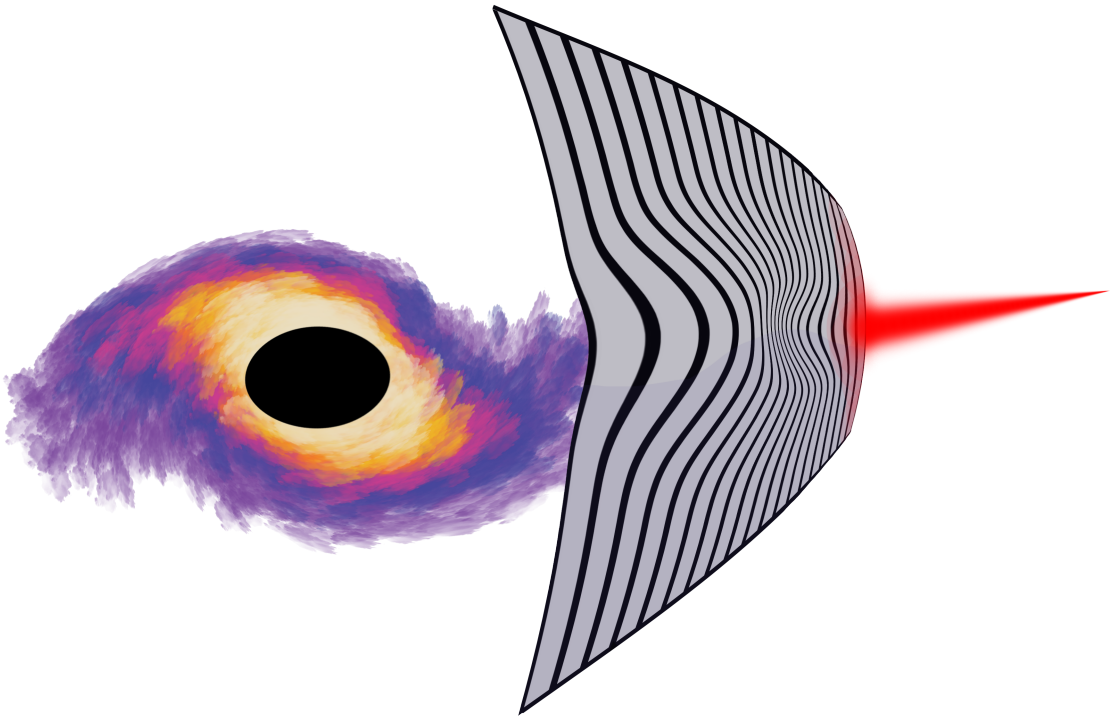

Surface Plasmon Polaritons in Strongly Correlated Media

A Holographic Approach

Master's thesis in Physics

ERIC NILSSON

DEPARTMENT OF PHYSICS

CHALMERS UNIVERSITY OF TECHNOLOGY

Gothenburg, Sweden 2021

www.chalmers.se

Master's thesis 2021

Surface Plasmon Polaritons in Strongly Correlated Media

A Holographic Approach

Eric Nilsson

CHALMERS
UNIVERSITY OF TECHNOLOGY

Department of Physics
Division of subatomic, high energy- and plasma physics
Chalmers University of Technology
Gothenburg, Sweden 2021

Surface Plasmon Polaritons in Strongly Correlated Media
A Holographic Approach
Eric Nilsson

Supervisor: Ulf Gran, Department of Physics
Examiner: Bengt E W Nilsson, Department of Physics

Master's Thesis 2021
Department of Physics
Division of subatomic, high energy- and plasma physics
Chalmers University of Technology
SE-412 96 Gothenburg
Telephone: +46 31 772 1000

Cover: Artist's illustration of a propagating surface plasmon polariton on the boundary of a the dual gravitational theory. Credit: Gustav Fjellheim Eriksson.

Typeset in LaTeX
Printed by Chalmers Reproservice
Gothenburg, Sweden 2021

Surface Plasmon Polaritons in Strongly Correlated Media
A Holographic Approach
Eric Nilsson
Department of Physics
Chalmers University of Technology

Abstract

The "strange metal" phase, exhibited by certain types of graphene and high-Tc superconductors above the transition temperature, sits at the frontier of condensed matter physics. However, successfully describing the phase proves to be a difficult task, as it is characterized by strong correlations, making conventional methods fail. Hence there is a need of novel approaches, where an alternative method comes from high-energy physics in the form of the holographic principle. It states that the strongly coupled theory can be mapped to a dual, weakly coupled, gravitational theory in one dimension higher, making calculations go from impossible to feasible. Surface plasmon polaritons (SPPs) are a valuable tool in an experimentalists toolbox, as they can serve as a probe of their surroundings. They may therefore useful in the design of the experiments needed to answer the questions about the strange metal phase. In this thesis, we model SPPs propagating on a strange metal in a holographic setting. By numerically solving unwieldy differential equations in the dual gravitational theory, with boundary conditions specified by the SPP system, we are able to obtain some numerical dispersion relations for the plasmons, although more work is needed. The results suggest that magnetic effects, which normally are suppressed, might come into play when the material is strongly correlated.

Keywords: plasmons, holographic duality, AdS/CFT, AdS/CMT, SPP

Acknowledgments

First of all I would like to express my deepest gratitude towards my supervisor Ulf Gran. I could not have wished for a better person to guide me along this thesis. Our lunches have been the weekly highlights during the last six months. Furthermore, Marcus Tornsö has provided tremendous help and very valuable discussions, for which I am very grateful.

I want to thank Bengt E W Nilsson, who not only has taught me most of the high-energy physics I know, but also encouraged me to look into the area of holography in condensed matter physics. I would not have ended up where I am without you!

Special thanks go also to my group of classmates that showed up to LB during the last year. You provided much needed social company in the isolating times of Covid-19.

Finally, a warm and grateful thank you to my family. You have always made sure that there is nothing else to worry about except the task at hand.

Eric Nilsson, Gothenburg, June 2021

Table of Contents

List of Figures

1. Introduction

Physics is the quest to explain nature. Due to the sheer complexity of the problems that physicists attempt to solve, there often is the need to use approximative methods. For instance, in perturbation theory, one considers corrections to a more simple, solvable problem. It works remarkably well, and is responsible for the most accurate prediction in all of physics. Calculations of the anomalous magnetic moment of the electron to tenth order in perturbation theory agrees with experiments to ten significant figures [1]! This can be attributed to the value of the fine structure constant, $\alpha \approx 1/137$, where the perturbative correction to the nth order contains n factors of the coupling constant, $\sqrt{\alpha}$. As such, higher-order terms contribute less and less[1], why the perturbation series can be truncated to obtain satisfactory results.

But what if the coupling constant would approach, or even exceed, unity? This is precisely what happens in *strongly correlated* systems, and the research of such systems sits at the frontier of both condensed matter and particle physics. Examples of systems that exhibit this behavior are the quark-gluon plasma, the state of matter in the very early Universe, and in so-called *strange metals*. As the name implies, these metals posses a multitude of exceptional properties. The most prominent feature is a linear-in-temperature resistivity, to be contrasted with the typical $\sim T^2$ result from Fermi liquid theory [3].

The strange metal phase appears in arguably two of the most interesting areas of condensed matter physics; namely in certain types of graphene [4] and in high-T_c[2] superconductors [5]. In the latter, the phase sits above the superconductive region in the phase diagram, extending all the way up to room temperature and beyond. The lack of a theoretical description therefore hinders any attempts of designing materials with a higher critical temperature, why an understanding of strange metals is paramount in order to reach the holy grail of room-temperature superconductivity.

Conventional methods in condensed matter physics rely on the existence of particle-like emergent phenomena called *quasiparticles*. But when the coupling is strong, the mean free path traveled by such "particles" becomes comparable to their de Broglie wavelength. This means that the state is very short-lived, so particle-like excitations are not well defined.

[1] In QED, which this relates to, there are details that need to be addressed. However, this does not affect the accuracy of practical calculations, see [2].

[2] Below the critical temperature T_c, the resistivity drops to zero. High-T_c superconductors have $T_c \geq 77\,\mathrm{K}$, the boiling point of nitrogen.

Furthermore, the strong coupling also challenges many numerical approaches, as numerical inaccuracies escalate, ruining the convergence of the numerics. Hence, there is a need of novel techniques able to handle the strongly coupled physics.

One promising method originates, maybe unexpectedly, from the theoretical physics community in their quest of a grand unified theory. The *AdS/CFT correspondence* in its original form relates two different limits of string theories, but has through the generalized notion of a *holographic duality* gained traction in the condensed matter community, where it is commonly called AdS/CMT[3]. It allows for an exploration of quantum many-body physics normally inaccessible by conventional techniques, serving as a way around the strongly coupled nature of e.g. strange metals. In short, the strongly coupled field theory is mapped to a dual, weakly coupled gravitational theory living in a higher dimension, making calculations go from impossible to feasible.

1.1 The AdS/CFT correspondence

The AdS/CFT correspondence (Anti-de Sitter/Conformal Field Theory) was first formulated by Juan Maldacena in 1997, and states that $\mathcal{N} = 4$ super Yang-Mills theory (a supersymmetric conformal field theory) in four-dimensional spacetime, has a dual description in terms of supergravity on $\mathrm{AdS}_5 \times S^5$ [6]. In the case of a generalized holographic duality, one instead considers a *large* N quantum field theory[4], dual to a *classical* gravitational theory in one dimension higher. The spacetime is only required to approach AdS as one moves towards its boundary, and the dual quantum field theory need not be conformal. One speaks of the gravitational theory as being in the *bulk*, whereas the dual field theory lives on the conformal *boundary* of the AdS spacetime. It is thorough this generalized duality that novel aspects of condensed matter systems may be explored.

The duality implies that physics inside of a volume can be described purely by information on its boundary, hence the name *holography*, akin to how a three-dimensional hologram is projected from information stored on a two-dimensional surface. The first hint of a holographic description was due to Hawking and Bekenstein, who realized that the entropy for a black hole is given by [7]

$$S_{\mathrm{HB}} = \frac{k_B A}{4\ell_p^2} \tag{1.1}$$

where k_B is the Boltzmann constant and ℓ_p the Planck length. This states that the entropy is related to the *area* A of the black hole, and not to its volume, as one would expect. Since black holes are maximally entropic objects, the result is striking, as it begs the question whether less entropic objects also can be described by boundary degrees of freedom.

The opposite viewpoint, where a lower dimensional theory has a dual description in a

[3] Anti-de Sitter/Condensed Matter Theory.

[4] N here refers to the degree of the gauge group, e.g. the strong force with gauge group $SU(3)$ has $N = 3$.

dimension higher, can be made sense of by considering the fact that the energy scale at which physical processes take place *does matter*. This is most explicitly seen in the running of coupling constants, where the value $\alpha \approx 1/137$ for the fine structure constant is only valid at the relatively low energies at which atomic physics takes place. At higher energies, such at those attained at the Large Hadron Collider, it has run to $\alpha \approx 1/127$ [8]. This process is called Renormalization Group (RG) flow, implying the existence of an extra scale parameter which controls the values of constants such as α. The holographic description in essence geometrizes the energy scale, where the extra dimension relates to the RG flow parameter of the boundary theory.

It should be noted that holographic duality is a conjecture. However, is has stood tall against numerous tests, to the point where it is now considered a "theorem", with an understanding comparable to that of the path integral [9].

1.2 Plasmons

A plasma is a gas-like substance made out of charged particles, and describes the conduction electrons in a normal metal, for instance. *Plasmons* are quanta of plasma oscillations, similar to how phonons are quanta of lattice oscillations, and may therefore be pictured as "electron sound waves". A *surface plasmon* is a special case of a plasmon, confined to an interface between a metal and a dielectric. This means that their properties are highly anisotropic, in contrast to normal *bulk* plasmons, which propagate through the entire material.

Plasmons are self-sustained oscillations, in the sense that they are solutions to Maxwell's equations in the absence of a source. However, they need to be excited somehow, akin to how a guitar string needs to be plucked in order to produce sound. In the case of surface plasmons, this is typically done by shining light on a metal, where the interaction of the photon with a plasmon produces a new type of quasiparticle — a *polariton*. When the frequency of the incident light matches the resonant surface plasmon frequency, it generates an electromagnetic wave propagating along the surface, referred to as a *surface plasmon polariton*, or SPP for short.

Although a theoretical description of plasmons did not come until until 1952 [10], they have long fascinated mankind. Their effects can often be seen in the visible part of the electromagnetic spectrum, explaining the colors of the stunning stained windows of the Notre-Dame and the dichroic glass[5] of the 4th-century Lycurgus cup. Furthermore, their optical effects are sensitive to changes in the surrounding environment, why research groups e.g. at Chalmers investigate the use of plasmonic nanoparticles in hydrogen sensors [11].

[5]This means that the color depends on the lighting conditions, i.e. whether the light is reflected or transmitted.

The study of plasmons in a strongly coupled setting has advanced, due to recent developments in experimental techniques. Momentum-resolved electron energy-loss spectroscopy (M-EELS) allows for precise measurement of the properties of plasmons in strange metals [12], probing the strongly correlated physics that traditional condensed matter theory is unable to explain. This motivates the pursuit of a holographic model, in order to construct an effective theory that can describe the behavior of the plasmons.

Gran et al. have previously investigated *bulk* plasmons in a strongly coupled setting using the holographic duality [13]–[15]. These papers use a model with two spatial dimensions, as is common, since the calculations become easier. A logical next step is therefore to increase the number of dimensions to three, where the effect of confinement to a two-dimensional surface, i.e. SPPs, may be investigated.

1.3 Outline of the thesis

This thesis tackles the modeling of surface plasmon polaritons using the holographic principle. The objective is twofold. Firstly, the holographic plasmon model will be extended to that of plasmons living in three spatial dimension, confined to a two-dimensional surface. Secondly, the dispersion relation for the holographic surface plasmon polaritons will be investigated.

Chapter 2 treats the holographic duality, and in detail covers the canonical example of a single scalar field in the bulk. The important relationships between bulk fields and boundary properties are formulated in a holographic dictionary. Chapter 3 studies the physics of surface plasmon polaritons, and derives the corresponding boundary conditions that make the holographic theory model SPPs in particular. The application of the holographic method to strongly correlated SPPs is outlined in Chapter 4, which step by step details the necessary calculations needed to obtain the dispersion relations. The equivalent of a conventional methods chapter is Section 4.4, which covers the the numerical implementation in Mathematica and Python. The results and conclusion follow in Chapters 5 and 6, respectively.

Appendix A illustrates the sign conventions used in this thesis, and contains short primers on mathematical concepts used. Appendix B is focused on detailed analytical calculations that are too long and cumbersome to be included in the main text.

A note on conventions
Calligraphic letters ($\mathcal{J}^\mu, \mathcal{A}_\mu, \mathcal{F}_{\mu\nu}$ etc.) will in general be used for fields in the boundary field theory, whereas normal letters are used for the bulk gravitational theory ($g_{\mu\nu}, A_\mu, F_{\mu\nu}$ etc.). Unless otherwise stated, "god-given" natural units $c = \hbar = 1$ are presumed and a mostly plus signature is used for the metric. For a detailed description where any minus signs show up, the reader is referred to Appendix A.2.

2. The Holographic Principle

In this chapter we cover the main machinery behind this thesis, namely the holographic principle. We will not detail Maldacena's original arguments that motivate the AdS/CFT correspondence, as this thesis mainly concerns AdS/CMT. The interested reader is referred to e.g. [9] or [16].

In order to illustrate the important *holographic dictionary*, which relates the physics on the boundary with the physics in the bulk, we walk through the canonical example of a single scalar field. This also allows us to obtain enough of an understanding so that the intricate steps in Chapter 4 become clear. The complete holographic dictionary can be found in A.1 for reference.

2.1 Anti-de Sitter space

The source-free Einstein's equations with a cosmological constant Λ,

$$R_{\mu\nu} - \frac{1}{2} g_{\mu\nu} \left(R - 2\Lambda \right) = 0, \tag{2.1}$$

admit three different maximally symmetric spacetime solutions; Minkowski, de Sitter and anti-de Sitter space, for $\Lambda = 0$, $\Lambda > 0$ and $\Lambda < 0$, respectively. D-dimensional Anti-de Sitter space (AdS_D) can be viewed as a hyperboloid embedded in a $(D+1)$-dimensional flat space with two time directions;

$$-X_0^2 - X_D^2 + X_i^2 = -L^2, \qquad i = 1, \dots D-1. \tag{2.2}$$

From this expression it is clear that the AdS length scale parameter L parametrizes the curvature of the space, akin to the radius of a sphere. The isometry group of AdS_D — the group of diffeomorphisms that leave the metric invariant — is $SO(2, D-1)$, as is manifest from the form of (2.2). This is but one of the hints of a duality to a conformal field theory, as $SO(2, D-1)$ is isomorphic to the conformal group in $D-1$ dimensions [17].

Using the constraint in (2.2) to solve for one of the degrees of freedom amounts to deter-

mining a specific coordinate system for AdS_D. A specific solution is on the form

$$\begin{aligned} X_D &= L\sqrt{1+\tan\varrho}\cos\tau \\ X_0 &= L\sqrt{1+\tan\varrho}\sin\tau \\ X_1 &= L\tan\varrho\cos\theta_1 \\ X_2 &= L\tan\varrho\sin\theta_1\cos\theta_2 \\ X_3 &= L\tan\varrho\sin\theta_1\sin\theta_2\cos\theta_3 \\ &\vdots \\ X_{D-2} &= L\tan\varrho\sin\theta_1\sin\theta_2\ldots\cos\theta_{D-2} \\ X_{D-1} &= L\tan\varrho\sin\theta_1\sin\theta_2\ldots\sin\theta_{D-2} \end{aligned} \tag{2.3}$$

where the ranges for the coordinates are $0 \leq \varrho \leq \pi/2$[1], $0 \leq \tau < 2\pi$, $0 \leq \theta_i < \pi$, $i = 1, \ldots, D-3$ and $0 \leq \theta_{D-2} < 2\pi$. The timelike coordinate τ is periodic but can be extended to the entirety of $\mathbb{R}$, giving the universal cover of AdS_D [9], which gives the AdS_D metric

$$\begin{gathered} \mathrm{d}s^2 = -\mathrm{d}X_0^2 - \mathrm{d}X_D^2 + \mathrm{d}X_i^2 \implies \\ \mathrm{d}s^2_{AdS_D} = \frac{L^2}{\cos^2\varrho}\left(-\mathrm{d}\tau^2 + \mathrm{d}\varrho^2 + \sin^2\varrho\,\mathrm{d}\Omega^2_{D-2}\right) \end{gathered} \tag{2.4}$$

where $\mathrm{d}\Omega^2_{D-2}$ is the metric on S^{D-2}. In these coordinates, it is apparent that the metric is topologically equivalent to a (hyper-)cylinder, which is a compact manifold, as seen in Figure 2.1. The part of AdS space that is mapped onto its boundary at $\varrho = \pi/2$, is called the *conformal boundary* of AdS space, where the conformal field theory will live, as we will motivate shortly.

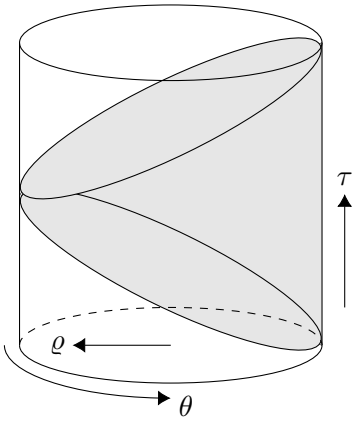

Figure 2.1: Illustration of the coordinate system (2.4) of AdS_3. For higher dimensions D, the circular part of the cylinder generalizes to a S^{D-2} topology. Shaded in gray is the Poincaré patch of AdS spacetime, and the conformal boundary is identified as the boundary of the cylinder.

Another set of coordinate transformations takes us to the *Poincaré* coordinates, where the

[1] This is valid for $D > 2$.

AdS_{d+2} metric reads

$$\mathrm{d}s^2 = \frac{L^2}{r^2}\left(-\mathrm{d}t^2 + \mathrm{d}x_d^2 + \mathrm{d}r^2\right) \tag{2.5}$$

where the conformal boundary now sits at $r = 0$. By restricting the radial coordinate to $r > 0$, only half of the AdS spacetime is covered. This is called the Poincaré patch, and shown in gray in Figure 2.1. We will later put a black hole in the interior, which cuts off the connection between the two parts anyway, why we let *the bulk* refer to the Poincaré patch of AdS space. It should be mentioned that the coordinate r is sometimes called z in the literature, with r being its inverse. However, since this thesis mainly concerns AdS_5, it is sensible to let $x_d = x, y, z$ denote the Cartesian three-dimensional coordinates while r corresponds to the extra dimension.

If we talk about the dual field theory being at the boundary, one could question how it can be affected by physics in the deep interior, which sits at $r = \infty$. However, AdS space enjoys the peculiar property that one can travel an infinite distance in finite time[2]. The dual field theory can therefore be seen as actually *living* on the boundary of AdS space, as it is causally connected to the entirety of the bulk.

Finally, the seemingly unintuitive choice of Poincaré coordinates where the boundary sits at $r = 0$ should be addressed. This is explained via the interpretation of the radial bulk coordinate r as the length scale of the boundary field theory. As energy is related to inverse length, we can think of the boundary IR physics as "residing" in the far interior ($r = \infty$) of the bulk, where one moves towards UV physics as $r \to 0$. Going from the gravity to the field theory side of the duality, one effectively integrates away the extra radial coordinate, reducing the number of dimensions. This represents a summation over higher order Feynman diagrams in perturbation theory, essentially geometrizing the Wilsonian renormalization group [18].

2.2 The holographic dictionary

Given a Lagrangian $\mathcal{L}$, the essential information of a quantum field theory can be encapsulated in a partition function, which is the path integral

$$Z_{\mathrm{QFT}}[h(x)] = \int \mathcal{D}\Phi\, \mathrm{e}^{\mathrm{i}\int \mathrm{d}^{d+1}x\,[\mathcal{L}+h(x)\mathcal{O}(x)]} \tag{2.6}$$

where Φ denotes the degrees of freedom of the quantum field. The term $h(x)\mathcal{O}(x)$ is called a *source term*, where $h(x)$ is an external field acting as a source for the local field operator $\mathcal{O}(x)$. Much like the partition function of statistical physics can be used to obtain thermodynamic quantities, the quantum field theoretical partition function allows for the calculation of the correlation functions of the theory. We say that that the partition

[2]More precisely, the proper distance is infinite, but the time it takes a photon to travel that distance is finite.

function is a *generating functional*. For instance, the one-point function (expectation value) of an operator is given by

$$\langle \mathcal{O} \rangle = \frac{1}{Z_0} \int \mathcal{D}\Phi \, \mathcal{O} \, \mathrm{e}^{\mathrm{i} \int \mathrm{d}^{d+1}x \, [\mathcal{L} + h(x)\mathcal{O}(x)]} = -\mathrm{i} \frac{1}{Z_0} \frac{\delta Z_{\mathrm{QFT}}}{\delta h(x)} \bigg|_{h(x)=0}, \tag{2.7}$$

where $Z_0 = Z_{\mathrm{QFT}}[h(x) = 0]$. Higher order n-point correlations functions are obtained in a similar fashion, by successively taking n variational derivatives of Z_{QFT} with respect to the operators' corresponding sources [19].

Gubser, Klebanov, Polyakov and Witten formulated a set of rules that relates the gravitational physics in the bulk with the boundary quantum field theory, called the *holographic dictionary*. Its cornerstone is the aptly named Gubser-Klebanov-Polyakov-Witten (GKPW) formula, which is an equality between the partition functions of the two different theories;

$$Z_{\mathrm{QFT}}[h(x)] = Z_{\mathrm{Grav}}[h(x)] \equiv \int^{\phi \to h} \mathcal{D}\phi \, e^{\mathrm{i}S_{\mathrm{Grav}}[\phi]}, \tag{2.8}$$

where, importantly, the boundary conditions for the bulk theory (represented as $\phi \to h$) corresponds to the source $h(x)$ of an operator $\mathcal{O}(x)$ in the boundary theory. Here ϕ can be any scalar, vector, spinor or tensor field, of which there can be multiple, each with their own boundary conditions. Just as the holographic duality itself, the formula is a conjecture. A derivation lies outside the scope even for most textbooks on the subject, so we will simply take it as a blessing from the heavens above.

As described in the introduction, the holographic duality implies that the QFT is described in the large N limit. This corresponds to stringy gravity reducing to classical gravity in the bulk, which means that the gravitational partition function can be evaluated semi-classically. By making a saddle-point approximation, the path integral can therefore be taken only along stationary ϕ [17]. Concretely, this means that it is valid to make the approximation

$$Z_{\mathrm{Grav}}[h(x)] = \mathrm{e}^{\mathrm{i}S_{\mathrm{Grav}}[\phi^*]} \tag{2.9}$$

where ϕ^* are solutions to the bulk equations of motion, subject to the boundary conditions $\lim_{r \to 0} \phi(x, r) = h(x)$. Applying the GKPW formula (2.8) then gives the expectation value of the boundary operator $\mathcal{O}$ in terms of the solutions to the bulk equations of motion as

$$\langle \mathcal{O} \rangle = -\mathrm{i} \frac{1}{Z_{\mathrm{QFT}}[0]} \frac{\delta Z_{\mathrm{QFT}}}{\delta h(x)} = \frac{\delta S_{\mathrm{Grav}}[\phi^*]}{\delta h(x)}. \tag{2.10}$$

It is in general not trivial to identify which boundary operator corresponds to what bulk field. However, they must without question respect the same symmetries, which allows for the identification of the most common pairs. A bulk scalar field ϕ corresponds to a boundary scalar operator (order parameter) $\mathcal{O}$. Furthermore, the bulk metric $g_{\mu\nu}$ corresponds to the energy-momentum tensor $T^{\mu\nu}$, while a bulk gauge field A_μ corresponds to a conserved symmetry current $\mathcal{J}^\mu$.

To keep track of the ideas discussed above, we condense the key takeaways in our own holographic dictionary:

Holographic dictionary

1. The partition functions of the $(d+2)$-dimensional gravitational theory and the dual $(d+1)$-dimensional QFT can be taken to be equal (the GKPW rule).
2. The source h of an operator $\mathcal{O}$ is the boundary value of the dual field.
3. A scalar operator $\mathcal{O}$ is dual to a scalar field ϕ in the bulk.
4. The boundary energy momentum tensor $T^{\mu\nu}$ is dual to the dynamical bulk metric $g_{\mu\nu}$.
5. A boundary conserved current $\mathcal{J}^{\mu}$ is dual to a bulk gauge field A_{μ}.

2.3 The canonical example

To illustrate how the the holographic dictionary can be used to relate quantities in the bulk and on the boundary, we consider the simplest possible case, namely that of a minimally coupled single scalar field ϕ in the bulk. The action for this system is

$$S = -\int \mathrm{d}^{d+2}x\,\sqrt{-g}\left(\frac{1}{2}(\partial^{\mu}\phi)(\partial_{\mu}\phi) + \frac{m^2}{2}\phi^2\right) \tag{2.11}$$

where g is the determinant of the metric $g_{\mu\nu}$. As an approximation, we neglect the backreaction of the scalar mass on the metric, i.e. that $g_{\mu\nu}$ is fixed and given by (2.5). Requiring that the action is stationary leads as expected to the massive wave equation in curved space;

$$\nabla^2\phi = m^2\phi \implies \phi'' - \frac{d}{r}\phi' + \left(\omega^2 - k^2 - \frac{m^2L^2}{r^2}\right)\phi = 0 \tag{2.12}$$

using a plane wave ansatz $\phi = \phi(r)\exp\{-\mathrm{i}\omega t + \mathrm{i}k\cdot x\}$, where we denote $\partial_r\phi = \phi'$. To investigate the behavior of the field near the boundary, we expand ϕ in a Laurent series with lowest exponent Δ as $\phi(r) = r^{\Delta} + \text{ h.o.t.}$ The differential equation then reads

$$\left[\Delta^2 - (d+1)\Delta - m^2L^2\right]r^{\Delta-2} + \left(\omega^2 + k^2 + \ldots\right)r^{\Delta} + \text{ h.o.t. } = 0. \tag{2.13}$$

Solving the equation to lowest order in r defines the *indicial equation* $I(\Delta) = 0$, where we find that

$$I(\Delta) = 0 \implies \Delta_{\pm} = \frac{d+1}{2} \pm \sqrt{\left(\frac{d+1}{2}\right)^2 + m^2L^2}, \tag{2.14}$$

where the two solutions are related as $\Delta_{\pm} = d + 1 - \Delta_{\mp}$. The radial part of the scalar field is as such given by a linear combination of the two solutions as

$$\phi(r \to 0) = \frac{\phi_{(0)}}{L^{d/2}}r^{\Delta_-} + \cdots + \frac{\phi_{(1)}}{L^{d/2}}r^{\Delta_+} + \ldots. \tag{2.15}$$

with $\phi_{(0)}$ and $\phi_{(1)}$ as the integration constants and factors of $L^{d/2}$ are factored out for later prettiness.

Before the GKPW rule (2.8) can be applied, we must investigate the finiteness of the on-shell action. When obtaining the equations of motion, we integrated (2.11) by parts. Due to the nature of AdS space, we need to take a closer look at the boundary term;

$$S = \frac{1}{2}\int_M \mathrm{d}^{d+2}x\,\sqrt{-g}\,\phi\left(\nabla^2 - m^2\right)\phi - \frac{1}{2}\oint_{\partial M}\mathrm{d}^{d+1}x\,\sqrt{-\gamma}\,\phi\, n^\mu\nabla_\mu\phi. \tag{2.16}$$

Here M is the bulk manifold, $\gamma_{\mu\nu} \equiv g_{\mu\nu} - n_\mu n_\nu$ is the induced metric on the boundary, and n^a is unit vector normal to the boundary which points out of the bulk, with the only non-zero component $n^r = -r/L$. At the conformal boundary ∂M, the volume diverges, why the theory needs to be regulated by placing the boundary at a finite cutoff radius $r = \epsilon$. With $\sqrt{-\gamma} = (L/\epsilon)^{d+1}$, the on-shell action reads

$$S^* = +\frac{1}{2}\oint_{r=\epsilon}\mathrm{d}^{d+1}x\left(\Delta_-\phi_{(0)}^2\epsilon^{2\Delta_- - d-1} + (d+1)\phi_{(0)}\phi_{(1)} + \Delta_+\phi_{(1)}^2\epsilon^{2\Delta_+ - d-1} + \ldots\right), \tag{2.17}$$

where the bulk term in (2.16) vanishes on-shell. The first term diverges as $\epsilon \to 0$, why the $\phi_{(0)}$ mode sometimes is referred to as *non-normalizeable* [20]. Similarly, we say that $\phi_{(1)}$ is a *normalizeable mode*. The divergence can be dealt with by adding a counterterm, which if purely is in terms of boundary data, will not affect the equations of motions in the bulk [17]. Either way, the counterterm clearly has to be Lorentz invariant, which severely limits the possible choices. The simplest non-trivial case is a ϕ^2 term, so by choosing a prefactor in order to cancel the non-normalizeable mode in (2.17), we let

$$S \to S + S_{\mathrm{ct}} = S - \frac{\Delta_-}{2L}\oint_{r=\epsilon}\sqrt{-\gamma}\,\phi^2. \tag{2.18}$$

The on-shell action now reads

$$S^* = \frac{1}{2}\oint_{r=\epsilon}\mathrm{d}^{d+1}x\,(\Delta_+ - \Delta_-)\phi_{(0)}\phi_{(1)} + \ldots \tag{2.19}$$

where higher order terms go to zero as $\epsilon \to 0$.

With this tidy form of the on-shell action in (2.19), the GKPW formula (2.10) can be used in order to calculate $\langle\mathcal{O}\rangle$. However, (2.14) tells us that Δ_- can be negative, meaning $\phi \to \infty$ as $r \to 0$, so how does one impose $\phi \to h$? The identification of r as the (inverse) energy scale, tells us that this corresponds to a UV divergence in the boundary theory, which needs to be regulated. This is precisely what we did in (2.18), but translated into a geometric language, where the divergence is due to the diverging volume of AdS space near the boundary.

To make sense of the boundary condition $\phi \to h$, we should therefore take the field theoretic source h as the leading order term $\phi_{(0)}$, which can be seen as the *renormalized* "boundary source" [9]. In the case presented above, this essentially means that

$$h(x) = \lim_{r\to 0}\phi(r)r^{-\Delta_-}L^{-d/2} = \phi_{(0)} \tag{2.20}$$

with the additional factors of L to compensate for the cosmetic surgery in (2.15)[3]. Additionally, the AdS metric (2.5) is invariant under a rescaling $\{t, x, r\} \to \lambda\{t, x, r\}$, so for solutions to the equations of motion, ϕ must also remain invariant. (2.15) therefore tells us that $\phi_{(0)} = h \to \lambda^{-\Delta_-} h$, so the action of "stripping off" factors of r in (2.20) is the implementation of renormalization group flow in λ, as taking $r \to 0$ can be seen as letting $\lambda \to 0$, i.e. flowing to the UV.

The variational derivative in (2.10) can now be taken:

$$\langle \mathcal{O} \rangle = \frac{\delta S[\phi^*]}{\delta h} = \frac{\Delta_+ - \Delta_-}{2} \frac{\delta}{\delta \phi_{(0)}} \left(\phi_{(0)} \phi_{(1)} \right) \tag{2.21}$$

where we note $\langle \mathcal{O} \rangle \sim \phi_{(1)}$. In the language of linear response theory, the response ($\mathcal{O}$) must be related to the source (h), why

$$\phi_{(1)} = \mathcal{C}\, \phi_{(0)} \tag{2.22}$$

where $\mathcal{C}$ in general will be a matrix for non-scalar fields. We therefore obtain the slightly peculiar result

$$\frac{\delta}{\delta \phi_{(0)}} \left(\phi_{(0)} \phi_{(1)} \right) = \phi_{(1)} + \phi_{(0)} \frac{\delta \phi_{(1)}}{\delta \phi_{(0)}} = \phi_{(1)} + \mathcal{C} \phi_{(0)} = 2\phi_{(1)}. \tag{2.23}$$

Finally, we arrive at an explicit expression for the expectation value of a boundary operator in terms of the bulk field as

$$\langle \mathcal{O} \rangle = (\Delta_+ - \Delta_-) \phi_{(1)}. \tag{2.24}$$

Since the source h scales as $h \to \lambda^{-\Delta_-} h$ under RG flow, and the measure on the boundary contains $d + 1$ factors of λ, the operator $\mathcal{O}$ conjugate to h must scale as

$$\mathcal{O}(x) \to \lambda^{-\Delta_+} \mathcal{O}(\lambda x) \quad \text{since} \quad -\Delta_+ = \Delta_- - d - 1, \tag{2.25}$$

in order for the boundary action to be invariant. This tells us that Δ_+ is the *scaling dimension* for the dual operator $\mathcal{O}$, in harmony with $\phi_{(1)}$ being the mode associated with the exponent Δ_+.

There is one caveat that should be mentioned; AdS space actually admits stable solutions for imaginary masses as long as $m^2 L^2 \geq -(d+1)^2/4$ [20], and (2.14) tells us that if $m^2 L^2 \leq 0$, both modes $\Delta_\pm$ are normalizeable. This allows one to interchange the roles of $\phi_{(0)}$ and $\phi_{(1)}$ in the regime $-(d+1)^2/4 \leq m^2 L^2 \leq 0$, called *alternative quantization*. This can be shown to correspond to a double trace deformation in the boundary theory, see e.g. [21].

[3] If there is conformal symmetry on the boundary, h can only be defined it up to scale transformations either way [9], so this does not really matter.

Holographic dictionary

6. If a source h is dual to a bulk field ϕ, it is canonically identified with the leading behavior of the solution ϕ^* to the bulk equations of motion.
7. The expectation value of the operator sourcing h is canonically identified with the sub-leading behavior of ϕ^*, and is explicitly calculated as $\langle \mathcal{O} \rangle = \frac{\delta S^*}{\delta h}$.
8. The exponent Δ_+ of the sub-leading solution is canonically identified as the scaling dimension of the boundary operator $\mathcal{O}$, and is dependent on the bulk field's mass.

To actually make the formula (2.24) useful, we must of course actually determine $\phi_{(1)}$, given $\phi_{(0)}$. To do so, we return to the equations of motion for the scalar field (2.12), and attempt to solve it throughout the entire bulk. A change of variables $\phi(r) = r^{\frac{d+1}{2}} y(r)$ and $x = \mathrm{i} r\sqrt{k^2 - \omega^2}$ leads to the Bessel equation

$$x^2 \frac{\mathrm{d}^2 y}{\mathrm{d}x^2} + x \frac{\mathrm{d}y}{\mathrm{d}x} + \left(x^2 - \alpha^2\right) y = 0, \tag{2.26}$$

where

$$\alpha^2 = m^2 L^2 + \frac{1}{4}(d+1)^2 = \Delta_+ - \frac{d+1}{2}. \tag{2.27}$$

Restricted to spacelike momenta, $k^2 > \omega^2$, this equation has the linearly independent solutions

$$y(x) = A\, I_\alpha(x) + B\, K_\alpha(x) \tag{2.28}$$

in terms of the modified Bessel functions

$$I_\alpha(x) = \sum_{m=0}^{\infty} \frac{1}{m!\Gamma(m+\alpha+1)} \left(\frac{x}{2}\right)^{2m+\alpha} \quad \text{and} \quad K_\alpha(x) = \frac{\pi}{2} \frac{I_{-\alpha}(x) - I_\alpha(x)}{\sin \alpha\pi}. \tag{2.29}$$

The solutions need to be regular in the interior, and since $I_\alpha(r) \to \infty$ as $r \to \infty$, we must require $A = 0$. Note that this does not mean that $\phi_{(1)}$ is zero — following (2.15), $\phi_{(1)}$ is the factor in front of r^{Δ_+}. However, the elimination of one of the independent constants effectively sets a relation between $\phi_{(0)}$ and $\phi_{(1)}$, i.e. *sets a relation between the source and its corresponding operator.* Hence there is a need to "do physics" in the bulk in order to determine $\langle \mathcal{O} \rangle$ using (2.10).

With the explicit expressions for the two solutions in (2.29), the retarded Green's function of the boundary theory (the two-point function) can be computed by taking yet another derivative of (2.10) with respect to the source. We find that

$$G^R_{\mathcal{O}\mathcal{O}}(\omega, k) \sim \frac{\delta \langle \mathcal{O} \rangle}{\delta h} \sim \frac{\phi_{(1)}}{\phi_{(0)}} \sim \left(k^2 - \omega^2\right)^{\Delta_+ - (d+1)/2} \tag{2.30}$$

which has the same form as a Green's function for a conformal scalar field with conformal dimension Δ_+ [9], in accordance with (2.25).

2.4 Trouble in AdS_5

For odd boundary space dimensions d, as will be the case for the plasmon system we wish to study, there are additional divergences that needs to be taken care of. To illustrate this, we return to the near-boundary Laurent series expansion of the scalar field, written in more detail as

$$L^{d/2}\phi = \phi_{(0)} r^{\Delta_-} \sum_{k=0}^{\infty} a_k r^k + \phi_{(1)} r^{\Delta_+} \sum_{k=0}^{\infty} b_k r^k. \tag{2.31}$$

Here $a_0 = b_0 = 1$ by definition, whereas higher order a_k, b_k are determined by solving (2.13) to successively higher orders in r. The form of (2.13) implies that all a_k and b_k with k odd vanish, in accordance with the full solutions (2.29). Hence higher order terms in the expansions of the solutions come with additional factors of r^2.

However, in the case of massless fields, (2.14) tells us that the solutions $\Delta_\pm$ are separated by even integers when d is odd. As such, there will come a point where the exponent of higher order terms in the expansion of the $\phi_{(0)}$ solution will be Δ_+, that of the second solution $\phi_{(1)}$. But since Δ_+ solves the indicial equation, it is impossible to satisfy the differential equation to order $r^{\Delta_+ - 2}$. The remedy is to add a logarithm to the term that degenerates as

$$a_{d+1} r^{d+1} \to a_{d+1} r^{d+1} \log r, \tag{2.32}$$

changing (2.31) to a *transseries* expansion. To illustrate how this solves the problem, consider a massless field in $d = 1$, such that $\Delta_\pm = 0, 2$. With the modified transseries expansion, (2.12) yields

$$\begin{aligned} \phi_{(0)} I(\Delta_-) r^{\Delta_- - 2} + \Big[\phi_{(0)} \left(\omega^2 + k^2 + a_2 \left[I(\Delta_-) \log r + 2\Delta_- - 2 \right] \right) \\ + \phi_{(1)} I(\Delta_+) \Big] r^{\Delta_+ - 2} + \mathcal{O}\left(r^{\Delta_+} \log r \right) = 0. \end{aligned} \tag{2.33}$$

Even though $I(\Delta_-) = I(\Delta_+) = 0$, a_2 can be determined such that that the differential equation is satisfied to next-to-leading order.

Since the logarithm diverges near the boundary, the action will require additional counterterms. Note that we technically committed a heinous crime by taking the logarithm of r, which is dimensionfull. Done properly, we would have to introduce a short-distance cutoff scale r_ϵ and write $\log(r/r_\epsilon)$. But this is only a problem if there is any residual $\log r$-dependence as seen from the boundary, so with a proper treatment of the boundary counterterm we can let this slip.

2.5 Black holes and temperature

When applying the holographic principle, there are primarily two different approaches. In "top-down" holography, one starts with a full string theory that is known to be UV complete, and that is a consistent theory of quantum gravity. This produces a conformally

invariant boundary theory, which is dual to a weakly coupled gravitational theory in the large N limit. However, condensed matter systems are typically not described by large N $SU(N)$ gauge theories, nor do they exhibit conformal invariance apart from critical points. Instead, we will start from a reasonable bulk action, and see what physics it can describe on the boundary. One might argue that this weakens the validity of the duality, and that the constructed theory might not be UV complete, but on the other hand, we obtain a boundary theory that actually describes the physics we are interested in — strongly coupled IR dynamics. This phenomenologically inclined approach is called "bottom-up" holography, and is the most common choice in the AdS/CMT setting [17]. Its usage is also supported by the fact that holographic duality can be motivated in the context of purely classical gravity, i.e. without introducing string theory [22].

In Section 2.3, we approximated the background to be static, as we were only interested in the scalar field and its connection to the boundary. In reality, the bulk action must of course yield equations of motion for the bulk metric $g_{\mu\nu}$ to which AdS space is a solution. In the case of bottom-up holography, stringy effects are essentially forgotten, meaning that the bulk is described by the Einstein-Hilbert action;

$$S_{\text{EH}} = \frac{1}{16\pi G}\int \mathrm{d}^{d+1}x\,\sqrt{-g}\,(R - 2\Lambda)\,, \tag{2.34}$$

where R is the Ricci scalar. Varying the action with respect to the dynamical metric $g_{\mu\nu}$ yields Einstein's equations (2.1), to which the static AdS metric (2.5) as a stable solution. The cosmological constant Λ is related to the AdS curvature as $-2\Lambda = d(d+1)/L^2$.

There are however more solutions than the static AdS solution to the Einstein-Hilbert action; namely black hole solutions. Furthermore, the holographic principle only requires that that the bulk is *asymptotically* AdS, that is, that the metric takes on the form (2.5) as $r \to 0$. We may therefore look for solutions with massive objects — black holes — in the interior of the bulk, as long as this condition is satisfied.

A black hole solution[4] to the equations of motion defined by (2.34) can be written as

$$\mathrm{d}s^2 = L^2\left(\frac{f(r)\mathrm{d}\tau^2}{r^2} + \frac{\mathrm{d}r^2}{f(r)r^2} + \frac{\mathrm{d}x_d^2}{r^2}\right) \tag{2.35}$$

where we have Wick rotated ($t \to -\mathrm{i}\tau$) to Euclidean space. In order for the space to be asymptotically AdS (the Euclidean version thereof), we demand that $f(0) = 1$. Furthermore, the Euclidean version of a black hole horizon is the statement $f(r_h) = 0$ for some horizon radius $r_h \geq 0$. An expansion the metric around $r = r_h$ gives the so-called cigar

[4]Technically a "black brane" solution, as the horizon will be planar. We will however still refer to it as a black hole, as is common in the literature.

geometry

$$\begin{aligned} \mathrm{d}s^2 &= L^2 \left(\frac{|f'(r_h)|(r_h - r)\mathrm{d}\tau^2}{r_h^2} + \frac{\mathrm{d}r^2}{|f'(r_h)|(r_h - r)r_h^2} + \frac{\mathrm{d}x_d^2}{r_h^2} \right) \\ &= \mathrm{d}\rho^2 + \rho^2 \mathrm{d}\varphi^2 + \frac{\mathrm{d}x_d^2}{r_h^2}, \quad r_h - r = \frac{r_h^2 |f'(r_h)|}{4}\rho^2, \quad \tau = \frac{2\varphi}{|f'(r_h)|}. \end{aligned} \tag{2.36}$$

Imposing that the spacetime is regular at the horizon means that we must identify $\varphi \sim \varphi + 2\pi$ in order to avoid the conical singularity at $\rho = 0$ [17]. The horizon has made the time coordinate φ periodic. The implications of this follow if we consider a quantum field theory at some finite temperature T. The quantum statistical partition function is

$$\begin{aligned} Z = \mathrm{tr}\left\{ \mathrm{e}^{-\beta H} \right\} &= \int \mathrm{d}^d q \, \langle q | \mathrm{e}^{-\beta H} | q \rangle = \left(\prod_{i=1}^{N} \int \mathrm{d}^d q_i \right) \langle q_1 | \mathrm{e}^{-\frac{\beta}{N} H} | q_2 \rangle \dots \langle q_{N-1} | \mathrm{e}^{-\frac{\beta}{N} H} | q_1 \rangle \\ &\xrightarrow{N \to \infty} \int \mathcal{D}q \exp\left\{ - \oint \mathrm{d}\tau \, \mathcal{L}_E(\tau) \right\} \end{aligned} \tag{2.37}$$

where $\beta = 1/k_B T$, H is the system Hamiltonian, q are generalized coordinates and $\mathcal{L}_E$ the Euclidean Lagrangian. Since the trace implies a summation over diagonal matrix elements, the product of transition matrix elements between neighboring states $\langle q_n |$ and $| q_{n+1} \rangle$ wraps around on itself, and we obtain a closed integral in the continuum limit, where the number of intermediate states N tends towards infinity. Importantly, the integral has period β, since $\mathrm{d}\tau = \beta/N$, meaning that *the periodicity in the time coordinate in Euclidean space is identified with the temperature for the field theory.*

The periodicity in φ can therefore be related to $\tau \sim \tau + 1/T$, which leads to the relation between the boundary temperature and the bulk metric

$$T = \frac{|f'(r_h)|}{4\pi}, \tag{2.38}$$

which is the Hawking temperature of the black hole [9]. Other thermodynamic quantities of the black hole translate to the boundary as well [9]. For instance, recall the Bekenstein-Hawking entropy in (1.1), which scales with the area of the black hole. In higher dimensions, the black hole entropy is generalized via the Ryu-Takayanagi formula [17], with the same key feature of being dependent on "area" and not volume. This means that from the boundary point of view, the entropy has the expected dimensional scaling, as the boundary theory lives in one dimension less.

Holographic dictionary

9. A finite temperature T on the boundary equals the Hawking temperature of a black hole in the bulk.

Note that the addition of temperature badly breaks the conformal symmetry of a scale invariant theory, described by the static AdS metric, at least in the IR. But this is exactly

what we want, as the physics of a real world condensed matter system is very much scale *dependent*: it depends on the energy of a process in relation to the ambient temperature. The fact that the effect of the black hole on the metric vanishes as $r \to 0$, captures that the boundary UV physics is unaffected by the temperature, where the conformal symmetry is regained. We can view the dual field theory as flowing from a scale invariant CFT in the UV, to a scale-dependent theory in the IR — the CMT in AdS/CMT.

2.6 Electromagnetism and chemical potential

If we are to model plasmons in holographic setting, we need to describe boundary electromagnetism. As is the case for most of bottom-up holographic condensed matter physics [17], we add a Maxwell term to the Einstein-Hilbert action, to obtain the *Einstein-Maxwell* action

$$S = S_{\text{EH}} - \frac{1}{4e^2}\int \mathrm{d}^{d+2}x\,\sqrt{-g}\,F_{\mu\nu}F^{\mu\nu}. \tag{2.39}$$

The bulk fields under consideration are therefore the dynamical metric $g_{\mu\nu}$ and the bulk gauge potential A_μ, related to the electromagnetic field tensor in the usual way as

$$F_{\mu\nu} = 2\nabla_{[\mu}A_{\nu]} = 2\partial_{[\mu}A_{\nu]} \equiv \partial_\mu A_\nu - \partial_\nu A_\mu \tag{2.40}$$

where ∇_μ is the covariant derivative defined by the metric $g_{\mu\nu}$[5].

In Section 2.2, we claimed that a bulk gauge field is dual to a conserved symmetry current on the boundary. Consider now the on-shell Maxwell part of the Einstein-Maxwell action, where the bulk gauge potential transforms as $A_\mu \to A_\mu + \nabla_\mu\alpha(x)$ under $U(1)$. Integrating the radial direction by parts, we find

$$\begin{aligned} S^* &\sim \oint_{\partial M} \mathrm{d}^{d+1}x\,\sqrt{-\gamma}n_r A_\mu F^{r\mu} \to \oint_{\partial M} \mathrm{d}^{d+1}x\,\sqrt{-\gamma}\,(A_\mu + \nabla_\mu\alpha)\,n_r F^{r\mu} \\ &= \oint_{\partial M} \mathrm{d}^{d+1}x\,\sqrt{-\gamma}\,(n_r A_\mu F^{r\mu} + \alpha\nabla_\mu n_r F^{r\mu})\,, \end{aligned} \tag{2.41}$$

integrating by parts on the boundary. As the bulk action is invariant under the gauge transformation,

$$\nabla_\mu n_r F^{r\mu}\Big|_{\delta M} \sim \nabla_\mu \mathcal{J}^\mu = 0, \tag{2.42}$$

so $\mathcal{J}^\mu$ is the conserved current on the boundary. Hence, A_μ is the holographic dual to the boundary current $\mathcal{J}^\mu$, why the corresponding source $\mathcal{A}_\mu$ should be obtained from the leading order terms from A^*_μ that solve the bulk equations of motion. Since A_μ is a gauge field, we are free to work in the *radial gauge* $A_r = 0$, making the mapping between components of A_μ and $\mathcal{A}_\mu$ one-to-one. Following the dictionary, we can therefore prescribe the identification

$$\lim_{r\to 0} A_\mu = \mathcal{A}_\mu \tag{2.43}$$

[5]Note that the simplification to normal partial derivatives *does not necessarily* hold when the indices are contravariant ($F^{\mu\nu}$)!

where A_μ may have to renormalized. Importantly, the incorporation of a bulk vector field allows us to model *compressible* phases of matter, that is, matter at some finite density [17]. This is tuned by a chemical potential μ on the boundary, the conjugate source to the charge density $\rho = \mathcal{J}^t$.

Holographic dictionary

10. The boundary and bulk vector potentials are identified as $\mathcal{A}_\mu = \lim_{r\to 0} A_\mu$.
11. A finite chemical potently μ on the boundary is the boundary value of the time component of the bulk vector potential.

With the close relation of $\mathcal{A}_\mu$ and A_μ, it follows that there is an electric field in the bulk, and Gauss' law implies this field must originate from somewhere. There are two alternatives: either there exists some type of charged matter in the bulk, or the black hole itself is charged. We will consider the latter, although there may be unstable behavior near the horizon [17], as the former is computationally very intricate (see e.g. [23]).

When the charge is "separated" between the boundary and the black hole, it is referred to as *fractionalized*. This is the case for the Reissner-Nordström black hole, the analogue of the Schwarzchild black hole solution to the Einstein-Maxwell action. Determining the AdS_5 version of the Reissner-Nordström black hole will be the first quest we seek out in Chapter 4.

With the Einstein-Maxwell action (2.39) and the identifications of the boundary temperature and chemical potential from (2.38) and (2.43), we have developed a holographic model that is dual to a static electromagnetic system at some specific ratio of μ/T. This is called the *Reissner-Nordström metal*, which attempts to model the strange metal. In order to realize surface plasmons of the strange metal, we have to find specific boundary conditions for the bulk fields. This is the topic of the next chapter.

3. Surface Plasmon Polaritons

This chapter treats the physics of surface plasmons polaritons, and defines the problem treated in this thesis. The main outcome is to obtain equations that serve as boundary conditions for the bulk fields. These boundary conditions are what makes a general holographic model describe the specific physical system of surface plasmon polaritons.

3.1 Plasmon and interface conditions

To find the defining equations for surface plasmons, we turn to Maxwell's equations in dielectric and magnetic media. Written in differential form[1], they read

$$\mathrm{d}\mathcal{F} = 0\,, \quad \mathrm{d}\star\mathcal{W} = \star\mathcal{J}_{\text{ext}}, \tag{3.1}$$

where $\mathcal{F} = \mathrm{d}\mathcal{A}$ is the electromagnetic field tensor, $\mathcal{W}$ is the induction tensor and $\mathcal{J}_{\text{ext}}$ is the external 4-current. These may without loss of generality be decomposed as

$$\begin{gathered}\mathcal{F} = \boldsymbol{\mathcal{E}} \wedge \mathrm{d}t + \star^{-1}(\boldsymbol{\mathcal{B}} \wedge \mathrm{d}t), \quad \mathcal{W} = \boldsymbol{\mathcal{D}} \wedge \mathrm{d}t + \star^{-1}(\boldsymbol{\mathcal{H}} \wedge \mathrm{d}t), \\ \mathcal{J}_{\text{ext}} = -\langle\rho_{\text{ext}}\rangle\,\mathrm{d}t + \boldsymbol{j}_{\text{ext}},\end{gathered} \tag{3.2}$$

where ρ_{ext} and $\boldsymbol{j}_{\text{ext}}$ is the external charge density and current, respectively.. The boldface denotes that the quantities are 3-vectors in space.

The electric field $\boldsymbol{\mathcal{E}}$ and the magnetic flux density $\boldsymbol{\mathcal{B}}$ are related to the displacement field $\boldsymbol{\mathcal{D}}$ and the magnetic field strength $\boldsymbol{\mathcal{H}}$ via the constitutive equations

$$\boldsymbol{\mathcal{D}} = \varepsilon_0\boldsymbol{\mathcal{E}} + \boldsymbol{\mathcal{P}} = \varepsilon_0\varepsilon\boldsymbol{\mathcal{E}} \quad \text{and} \quad \boldsymbol{\mathcal{B}} = \mu_0\left(\boldsymbol{\mathcal{H}} + \boldsymbol{\mathcal{M}}\right) = \mu_0\mu\boldsymbol{\mathcal{H}}. \tag{3.3}$$

where $\boldsymbol{\mathcal{P}}$ and $\boldsymbol{\mathcal{M}}$ are the polarization and magnetization inside of the material, respectively [24]. These equations also define the dielectric function ε and the permeability μ (not to be confused with the chemical potential) which characterize the material. ε_0 and μ_0 are the vacuum permittivity and permeability, respectively, related to the speed of light as $c^{-2} = \varepsilon_0\mu_0$. With the decompositions in (3.2), Maxwell's equations (3.1) can be expressed in the more familiar vector form;

$$\begin{aligned}\nabla\cdot\boldsymbol{\mathcal{B}} &= 0, & \nabla\cdot\boldsymbol{\mathcal{D}} &= \rho_{\text{ext}}, \\ \nabla\times\boldsymbol{\mathcal{E}} &= -\frac{\partial\boldsymbol{\mathcal{B}}}{\partial t}, & \nabla\times\boldsymbol{\mathcal{H}} &= \boldsymbol{j}_{\text{ext}} + \frac{\partial\boldsymbol{\mathcal{D}}}{\partial t}.\end{aligned} \tag{3.4}$$

[1] For a short primer on the language of exterior calculus and differential forms, see Appendix A.3.

In order to realize a surface plasmon, we consider the most basic setup consisting of a metal slab surrounded by a dielectric with constant and real permittivity ε_1, as shown in Figure 3.1. The coordinate system is chosen such that the interface between the two media is situated at $z = 0$, and without loss of generality, the electromagnetic wave is assumed to propagate along the x-direction. Idealizing a real-world setup, the metal slab is assumed to extend infinitely in the x-y plane and down to $z = -\infty$.

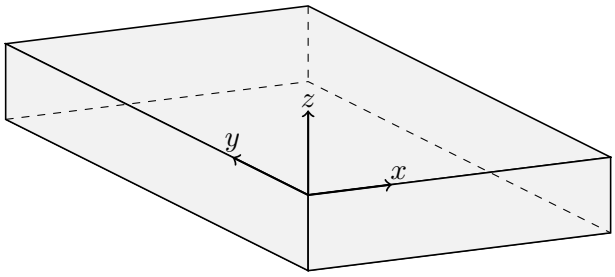

Figure 3.1: The surface plasmons are confined to the interface between a dielectric ($z > 0$) with constant and real permittivity ε_1 and a (strange) metal ($z < 0$) with an undetermined dielectric function $\varepsilon(\omega, \boldsymbol{k})$. The plasmons propagate in the x-direction.

We begin the analysis within the dielectric, for $z > 0$, and look for solutions to the electric and magnetic fields $\boldsymbol{\mathcal{E}}$ and $\boldsymbol{\mathcal{H}}$. A plasmon is a collective oscillation where the excitations are self-sustained, i.e. solutions to Maxwell's equations without external sources ($\mathcal{J}_{\text{ext}} = 0$) [24]. This means that the curl equations in (3.4) can be combined as

$$\nabla \times \nabla \times \boldsymbol{\mathcal{H}} = -\frac{\varepsilon_1}{c^2}\frac{\partial^2 \boldsymbol{\mathcal{H}}}{\partial t^2} \tag{3.5}$$

whereby the vector identity $\nabla^2 \boldsymbol{\mathcal{H}} = \nabla(\nabla \cdot \boldsymbol{\mathcal{H}}) - \nabla \times \nabla \times \boldsymbol{\mathcal{H}}$ leads to a wave equation for the magnetic field,

$$\nabla^2 \boldsymbol{\mathcal{H}} - \frac{\varepsilon_1}{c^2}\frac{\partial^2 \boldsymbol{\mathcal{H}}}{\partial t^2} = 0. \tag{3.6}$$

assuming there is no source for magnetization in the dielectric, i.e. $\mu_1 = 1$.

Surface plasmons normally come only from transverse magnetic (TM) modes, where the magnetic field transverse to the direction of propagation. Systems with non-unity magnetization μ can support transverse electric (TE) modes as well, but the two types of modes are decoupled [25]. We will restrict ourselves to the study of TM modes, so from the shape of the wave equation, we make a plane wave ansatz decaying in the z-direction for the vector potential as

$$\mathcal{A}^{(1)} = \left(\alpha_x^{(1)}\mathrm{d}x + \alpha_z^{(1)}\mathrm{d}z\right)\mathrm{e}^{-\mathrm{i}\omega t + \mathrm{i}kx - \lambda_1 z} \tag{3.7}$$

where the reciprocal value of the attenuation constant, $1/|\lambda_1|$, defines the evanescent decay into the dielectric, and the wavevector is $\boldsymbol{k} = (k, 0, \mathrm{i}\lambda_1)$. Assuming that the dielectric is non-magnetizing ($\mu_1 = 1$), the electric and magnetic fields follow directly from the vector

potential ansatz as

$$\begin{aligned}\boldsymbol{\mathcal{E}}^{(1)} &= \left(\mathrm{i}\omega\alpha_x^{(1)}\mathrm{d}x + \mathrm{i}\omega\alpha_z^{(1)}\mathrm{d}z\right)\mathrm{e}^{-\mathrm{i}\omega t+\mathrm{i}kx-\lambda_1 z}\\ \boldsymbol{\mathcal{H}}^{(1)} &= -\frac{1}{\mu_0}\left(\lambda_1\alpha_x^{(1)} + \mathrm{i}k\alpha_z^{(1)}\right)\mathrm{d}y\,\mathrm{e}^{-\mathrm{i}\omega t+\mathrm{i}kx-\lambda_1 z}\end{aligned} \tag{3.8}$$

where the displacement field is trivially related to the electric field as $\boldsymbol{\mathcal{D}} = \varepsilon_0\varepsilon_1\boldsymbol{\mathcal{E}}$. Inserting the ansatz for $\boldsymbol{\mathcal{H}}$ into the wave equation (3.6) directly relates the attenuation λ_1 to the other parameters,

$$k^2 - \lambda_1^2 = \mu_0\varepsilon_0\varepsilon_1\omega^2. \tag{3.9}$$

This is simply is the statement that the electromagnetic wave is light-like with the speed of light modified by the material, i.e.

$$k_\mu k^\mu = 0, \quad \text{where} \quad k_\mu = (-\sqrt{\varepsilon_1}\frac{\omega}{c}, k, 0, -\mathrm{i}\lambda_1). \tag{3.10}$$

Note that in general, $\omega, k \in \mathbb{C}$, where the imaginary part models the diffusive behavior. However, we can always choose to take one of them real, and consider decay in either time or space only.

Inside the metal, for $z < 0$, we assume that the system is strongly coupled and that $\varepsilon_2 = \varepsilon(\omega, \boldsymbol{k})$ is non-trivial. In order to account for any unexpected behavior of strongly coupled physics, we make no prior assumptions on $\mu_2 = \mu(\omega, \boldsymbol{k})$, which means that we do not assume the existence of a simple wave equation for the fields. Still considering TM modes, an analogous ansatz for the vector potential reads

$$\mathcal{A}^{(2)} = \left(\alpha_x^{(2)}\mathrm{d}x + \alpha_z^{(2)}\mathrm{d}z\right)\mathrm{e}^{-\mathrm{i}\omega t+\mathrm{i}kx+\lambda_2 z}, \tag{3.11}$$

where again, $1/|\lambda_2|$ defines the evanescent decay, this time into the metal. However, with non-trivial permeability, it is convenient to make a separate ansatz for the magnetic field as

$$\boldsymbol{\mathcal{H}}^{(2)} = h_y\mathrm{d}y\,\mathrm{e}^{-\mathrm{i}\omega t+\mathrm{i}kx+\lambda_2 z}. \tag{3.12}$$

The displacement field then follows from Maxwell's equations, as

$$\boldsymbol{\mathcal{D}}^{(2)} = \frac{h_y}{\omega}\left(-\mathrm{i}\lambda_2\mathrm{d}x - k\mathrm{d}z\right)\mathrm{e}^{-\mathrm{i}\omega t+\mathrm{i}kx+\lambda_2 z}, \tag{3.13}$$

but might not be trivially related to $\boldsymbol{\mathcal{E}}^{(2)}$, as the assumption about μ being non-trivial might make ε a non-diagonal matrix.

The different solutions can now be related across the interface at $z = 0$. Maxwell's equations implies that the normal component of displacement field and the transverse components of the electric and magnetic field have to be continuous[2], which leads to the matching conditions

$$\boldsymbol{\mathcal{E}}_x^{(1)} - \boldsymbol{\mathcal{E}}_x^{(2)}\Big|_{z=0} = 0\,, \quad \boldsymbol{\mathcal{D}}_z^{(1)} - \boldsymbol{\mathcal{D}}_z^{(2)}\Big|_{z=0} = 0\,, \quad \boldsymbol{\mathcal{H}}_y^{(1)} - \boldsymbol{\mathcal{H}}_y^{(2)}\Big|_{z=0} = 0\,. \tag{3.14}$$

[2]This is valid as long as there is no external surface charge or current, respectively

Inserting the above ansätze, the matching conditions reads

$$\alpha_x^{(1)} = \alpha_x^{(2)}, \quad \mathrm{i}\omega\varepsilon_0\varepsilon_1\alpha_z^{(1)} = -\frac{k}{\omega}h_y, \quad \lambda_1\alpha_x^{(1)} + \mathrm{i}k\alpha_z^{(1)} = -\mu_0 h_y, \tag{3.15}$$

which when combined with the wave equation in the dielectric (3.9), leads to the defining surface plasmon *interface condition*

$$\varepsilon_0\varepsilon_1\omega^2\alpha_x - \sqrt{k^2 - \varepsilon_0\mu_0\varepsilon_1\omega^2}h_y = 0, \tag{3.16}$$

dropping the superscript on α_x. The magnetic field y-component h_y can be obtained from difference between the magnetic flux density and the magnetization as

$$\mathcal{H}_y^{(2)} = \frac{1}{\mu_0}\mathcal{B}_y^{(2)} - \mathcal{M}_y = \frac{1}{\mu_0}\left(\partial_z\mathcal{A}_x^{(2)} - \partial_x\mathcal{A}_z^{(2)}\right) - \mathcal{M}_y. \tag{3.17}$$

This means that the interface condition can be written purely in terms of the boundary vector field and magnetization as

$$\omega^2\mathcal{A}_x - \sqrt{k^2 - \omega^2}\left(\lambda_2\mathcal{A}_x - \mathrm{i}k\mathcal{A}_z - \mathcal{M}_y\right) = 0 \tag{3.18}$$

in units where $c = 1$, and where the relative permittivity of the dielectric is set to $\varepsilon_1 = 1$ (e.g. air). The discussion of the boundary magnetization follows in the next section.

With the plane wave ansätze for the fields inside of the metal, Maxwell's equations can be rewritten into a more useful form. The current is related to the field strength and induction tensor as [14]

$$\mathrm{d}\star(\mathcal{F} - \mathcal{W}) = \star\mathcal{J}. \tag{3.19}$$

Zero external current means that $\mathrm{d}\star\mathcal{W} = 0$ inside of the strange metal, so we are left with

$$\mathrm{d}\star\mathcal{F} = \star\mathcal{J} \implies \nabla\times\boldsymbol{\mathcal{B}} - \frac{\partial\boldsymbol{\mathcal{E}}}{\partial t} = \boldsymbol{j}. \tag{3.20}$$

Using the relation $\boldsymbol{\mathcal{E}} = -\partial_t\mathcal{A}_i - \nabla\mathcal{A}_t$, we find for the x-component that

$$\left(\omega^2 + \lambda_2^2\right)\mathcal{A}_x + \omega k\mathcal{A}_t - \mathrm{i}k\lambda_2\mathcal{A}_z + \mathcal{J}_x = 0, \tag{3.21}$$

and similarly for the z-component;

$$\left(\omega^2 - k^2\right)\mathcal{A}_z - \mathrm{i}k\lambda_2\mathcal{A}_x - \mathrm{i}\omega\lambda_2\mathcal{A}_t + \mathcal{J}_z = 0. \tag{3.22}$$

Following [13], these two equations will be referred to as the *plasmon conditions*, as they in the case of $\lambda_2 = 0$ imply the existence of bulk plasmons.

3.2 Magnetization through holography

The interface condition (3.14) contains the boundary magnetization $\mathcal{M}_y$, which needs to be modeled holographically. Just as the chemical potential μ is the thermodynamic conjugate to the charge density ρ, the magnetization (density) $\mathcal{M}$ is conjugate to the

magnetic flux density $\mathcal{B}$. The holographic dictionary therefore implies that $\mathcal{M}$ is obtained by taking a variational derivative of the on-shell bulk action with respect to $\mathcal{B}$ [26].

Consider the Maxwell part of the bulk action. Written in terms of differential forms, it reads

$$S_M = \int_M F \wedge *F \tag{3.23}$$

where F is the bulk electromagnetic 2-form and $*$ is the 5-dimensional Hodge operator in the bulk. We assume the existence of a *homotopy operator* $\mathcal{K}$ which satisfies

$$\omega = \mathcal{K}\mathrm{d}\omega + \mathrm{d}\mathcal{K}\omega \quad \text{and} \quad \iota_n \mathcal{K} = 0 \text{ on } \partial M \tag{3.24}$$

for a form ω. The homotopy operator may be constructed via radial integration, since AdS_5 is naturally foliated into parallel submanifolds (surfaces of constant r) [27]. Since the magnetic flux density $\mathcal{B}$ is related to the vector potential $\mathcal{A}$ via a derivative, consider the contributions to the variation of the action from $\delta(\mathrm{d}A)$;

$$\delta S = \int_M \delta(\mathrm{d}A) \wedge *F = \oint_{\partial M} \delta(\mathrm{d}A) \wedge \mathcal{K} * F \tag{3.25}$$

using (3.24) and Stokes' theorem. The details of this calculation can be found in Appendix A.4. Since the bulk and boundary vector potentials are directly identified, $\mathrm{d}A\big|_{\partial M} = \mathrm{d}\mathcal{A} = \mathcal{F}$, so the variational derivative with respect to $\mathcal{B}_y = \mathcal{F}_{zx}$ yields the ty component of $\mathcal{K} * F$. We may therefore construct a bulk field M_y as

$$M_y(r) = \left\langle \int_{r_h}^{r} *F,\, \mathrm{d}y \wedge \mathrm{d}t \right\rangle = \int_{r_h}^{r} \mathrm{d}r \, (\partial_x A_z - \partial_z A_x) \tag{3.26}$$

where the boundary magnetization is identified as $\mathcal{M}_y = \lim_{r\to 0} M_y$.

4. Holography in Action

The computational prowess defined by the holographic framework in Chapter 2 and the model specific boundary conditions in Chapter 3 are now ready to be combined. This chapter outlines all the necessary calculations from the dual gravitational point of view. Starting from a bulk action, we end up with an optimization problem which may be solved for in order to obtain the dispersion relation for the plasmons. Most of the calculations take help of Mathematica [28], and in particular the `xAct` package [29], as they are unreasonable to do by hand. The Mathematica notebook may be requested by contacting the author.

4.1 Background solutions

The starting point is the Einstein-Maxwell action

$$S_0 = \int \mathrm{d}^5x \sqrt{-g} \left(\frac{R}{2} - \Lambda - \frac{1}{4} F_{\mu\nu} F^{\mu\nu} \right) \tag{4.1}$$

where R is the Ricci scalar of the manifold defined by the metric $g_{\mu\nu}$. For simplicity, we have chosen units where $8\pi G = 1$ and absorbed the constant e into the vector potential. As we saw in Section 2.3, the action may need to be renormalized, but this will not affect the bulk equations of motion. Hence we can vary the bare action S_0 with respect to the metric and vector potential, yielding the Einstein's and Maxwell's equations of motion;

$$\begin{aligned} \delta g_{\mu\nu} :&\ 0 = -\Lambda g^{\mu\nu} - \frac{1}{4} g^{\mu\nu} F_{\kappa\lambda} F^{\kappa\lambda} + F^{\mu\kappa} F^{\nu}{}_{\kappa} - R^{\mu\nu} + \frac{1}{2} g^{\mu\nu} R \\ \delta A_\mu :&\ 0 = \nabla_\kappa \nabla^\kappa A^\mu - \nabla_\kappa \nabla^\mu A^\kappa \end{aligned} \tag{4.2}$$

both of which are nonlinear. This is remedied by linearizing the equations, i.e. considering small perturbations around a static background solution.

Under the assumption that the background is homogeneous and isotropic in space, and static in time, we make ansätze for the metric and vector potential as

$$\mathrm{d}s^2 = \frac{L^2}{r^2} \left(-f(r)\mathrm{d}t^2 + \mathrm{d}x_i^2 + g(r)\mathrm{d}r^2 \right) \quad \text{and} \quad A_\mu = L \left(h(r), 0, 0, 0, 0 \right), \tag{4.3}$$

introducing three unknown scalar functions f, g and h. The metric ansatz generalizes the pure AdS metric (2.5), and the vector potential ansatz respects our choice of radial gauge. Furthermore, a static background solution corresponds to a static, unperturbed system on the field theory side. This means that both the bulk vector potential and some higher order derivative of it mush vanish at the boundary, ensuring that the boundary

electromagnetic field is static. It is therefore suitable to consider a background solution with only a non-zero time component, since it relates to the boundary chemical potential, μ.

Inserting the ansätze into the equations of motion (4.2) allows relates the scalar functions by the following equations:

$$\begin{aligned} 0 &= -12f + 12fg + 3rf' - r^4 h'^2 \\ 0 &= 12fg - 12fg^2 + 3frg' + gr^4 h'^2 \\ 0 &= rh'' - h'. \end{aligned} \tag{4.4}$$

The solutions to the two first order and one second order differential equations have four degrees of freedom, which we suggestively denote μ, c, M and Q. Introducing the black hole horizon $r = r_h$ as the characteristic length scale, the solution to the equation for $h(r)$ can be written as

$$h(r) = \mu - \sqrt{\frac{3}{2}} Q \left(\frac{r}{r_h} \right)^2. \tag{4.5}$$

Following our discussion around (2.43), the integration constant μ really is the chemical potential of the boundary. Furthermore, the holographic dictionary tells us that the boundary charge density $\langle \mathcal{J}^t \rangle = \rho$ is obtained from the subleading term in the near-boundary expansion of A_t, so Q must be some function of ρ. From the bulk point of view, the charge can only originate from the only object there is; namely the black hole[1], so we identify Q as the charge of the Reissner-Nordström black hole. In order to avoid a gauge singularity, the vector potential must vanish at the horizon, $h(r_h) = 0$ [17], which sets the relation between the boundary chemical potential charge density, dependent of the black hole radius r_h.

We continue with μ as the free parameter of choice, after which the solutions to the remaining equations read

$$\begin{aligned} f(r) &= c^2 - M \frac{r^4}{r_h^3} + \frac{2\mu^2}{3} \frac{r^6}{r_h^4} \\ g(r) &= \frac{c^2}{f(r)}. \end{aligned} \tag{4.6}$$

With our choice of units, the speed of light is unity, so at the boundary where the metric should asymptote to free AdS space, we must require $f(0) = 1$, i.e. $c = 1$. Just like in Section 2.5, there is another constraint on $f(r)$ at the horizon, as it is defined by $f(r_h) = 0$. This allows us to specify the remaining parameter M, interpreted as the mass of the black hole, such that $r_h = 1$ (length units) via

$$M = \frac{1}{3} \left(3 + 2\mu^2 \right) \tag{4.7}$$

[1]Since we chose to study fractionalized charge.

meaning that the finalized background solutions read

$$\begin{aligned} h(r) &= \mu(1-r^2) \\ f(r) &= 1 - \left(1 + \frac{2\mu^2}{3}\right) r^4 + \frac{2\mu^2}{3} r^6 \\ g(r) &= \frac{1}{f(r)}. \end{aligned} \tag{4.8}$$

However, let us keep the factors of r_h explicit and investigate the temperature, akin to Section 2.5. Avoiding the conical singularity at the horizon now yields a slightly more intricate expression;

$$T = \frac{3 - \mu^2 r_h^2}{3\pi r_h}. \tag{4.9}$$

We may construct a dimensionless parameter quantifying the *scale* of the system, as the ratio of the chemical potential to the temperature as

$$\frac{\mu}{T} = \frac{3\pi\hat{\mu}}{3 - \hat{\mu}^2} \tag{4.10}$$

where μ is explicitly made dimensionless as $\hat{\mu} = \mu r_h$. This expression also clearly illustrates the bound $\hat{\mu} < \sqrt{3}$, and approaching it means that the temperature of the black hole approaches zero. A zero-temperature black hole is possible in the Reissner-Nordström case, and happens when the entirety of the black hole's mass comes from its electromagnetic energy [9]. Since charge is conserved, the black hole cannot radiate, which is equivalent to the statement that its Hawking temperature is zero.

Analogously, we can express the fractions of other dimensionfull parameters to the temperature as

$$\frac{k}{T} = \frac{3\pi\hat{k}}{3 - \hat{\mu}^2}, \qquad \frac{\omega}{T} = \frac{3\pi\hat{\omega}}{3 - \hat{\mu}^2}, \qquad \frac{\lambda_2}{T} = \frac{3\pi\hat{\lambda}_2}{3 - \hat{\mu}^2}. \tag{4.11}$$

where $\hat{k} = k r_h$, $\hat{\omega} = \omega r_h$ and $\hat{\lambda}_2 = \lambda_2 r_h$ are dimensionless.

4.2 Perturbative solutions

We have now managed to describe the bulk space corresponding to a static boundary system, at some finite temperature T and chemical potential μ, via the background solutions (4.8). But in order to realize plasmons traveling along the interface, the system needs to be excited somehow. In an experimental setting this would typically be done by shining a laser onto the surface, which given the correct frequency can excite a surface plasmon polariton.

Excitations in the bulk are modeled by considering small perturbations of the background solution as $g_{\mu\nu} \to g_{\mu\nu} + \delta(g_{\mu\nu})$ and $A_\mu \to A_\mu + \delta(A_\mu)$, in line with the linearization of the equations of motion. More precisely, we perturb the metric, following the plane wave

ansatz in Section 3.1, as

$$\delta(g_{\mu\nu}) = \epsilon\frac{L^2}{r^2}\mathrm{e}^{-\mathrm{i}\omega t+\mathrm{i}kx+\lambda_2 z}\begin{pmatrix} \delta g_{tt}(r) & \delta g_{tx}(r) & \delta g_{ty}(r) & \delta g_{tz}(r) & 0 \\ \delta g_{tx}(r) & \delta g_{xx}(r) & \delta g_{xy}(r) & \delta g_{xz}(r) & 0 \\ \delta g_{ty}(r) & \delta g_{xy}(r) & \delta g_{yy}(r) & \delta g_{yz}(r) & 0 \\ \delta g_{tz}(r) & \delta g_{xz}(r) & \delta g_{yz}(r) & \delta g_{zz}(r) & 0 \\ 0 & 0 & 0 & 0 & 0 \end{pmatrix} \tag{4.12}$$

where ϵ is a small parameter, effectively determining the size of the perturbation. L^2/r^2 is factored out in order to account for the diverging shape of the metric as $r \to 0$, which makes it meaningful to impose boundary conditions for the fluctuations $\delta g_{\mu\nu}$. Furthermore, since $g_{\mu\nu}$ is a gauge field just like A_μ, we can choose a radial gauge such that we only consider diffeomorphisms that leave the radial parts of the metric invariant. Thus, in order to stay in gauge, we set $\delta g_{\mu r} = 0$.

In a similar fashion, the vector potential is perturbed as

$$\delta(A_\mu) = \epsilon L\mathrm{e}^{-\mathrm{i}\omega t+\mathrm{i}kx+\lambda_2 z}(\delta A_t, \delta A_x, \delta A_y, \delta A_z, 0) \tag{4.13}$$

where $\delta A_r = 0$ respects the choice of radial gauge. We define

$$\Phi \equiv \{\delta g_{tt}, \ldots, \delta A_t, \ldots, \delta A_z\}, \tag{4.14}$$

containing the 14 different *fluctuations* (to be distinguished from the perturbations, defined via the expressions in (4.12) and (4.13)).

Inserting the perturbations into the action yields

$$S = S^{(0)} + \epsilon S^{(1)} + \epsilon^2 S^{(2)} + \mathcal{O}\left(\epsilon^3\right) \tag{4.15}$$

where $S^{(0)}$ determines the background equations which are solved by (4.8), and the equations of motion defined by $S^{(1)}$ is zero by solutions to the background, as will be shown later. $S^{(2)}$ defines the linearized equations of motion for the fluctuations, which in total amounts to a system of coupled differential equation on the form

$$\begin{aligned} D_1(\Phi) &= 0 \\ &\vdots \\ D_{14}(\Phi) &= 0 \end{aligned} \tag{4.16}$$

which we will refer to as the *fluctuation equations*. Here D_i, $i = 1, \ldots, 14$ are intricate second order differential operators, the exact form of which depends on the background solutions. For instance, the x-component of the bulk Maxwell's equations reads

$$\begin{aligned} D_{12}(\Phi) = (\delta A_x)'' + \frac{h'}{f}(\delta g_{tx})' + \left(\frac{f'}{f} - \frac{1}{r}\right)(\delta A_x)' \\ + \frac{rh'' - h'}{fr}\delta g_{tx} + \frac{\omega k}{f^2}\delta A_t + \frac{\omega^2 + \lambda_2^2 f}{f^2}\delta A_x - \frac{\mathrm{i}k\lambda_2}{f}\delta A_z = 0. \end{aligned} \tag{4.17}$$

The transverse sector, consisting of $\Phi_T = \{\delta g_{ty}, \delta g_{xy}, \delta g_{yz}, \delta A_y\}$, decouples from the longitudinal sector

$$\Phi_L = \{\delta g_{tt}, \delta g_{xx}, \delta g_{yy}, \delta g_{zz}, \delta g_{tx}, \delta g_{tz}, \delta g_{xz}, \delta A_t, \delta A_x, \delta A_z\}\,, \tag{4.18}$$

since the linear equations are invariant under the parity transformation $y \to -y$ in the longitudinal sector, but not in the transverse sector. Plasmons are in general longitudinal waves, why their behavior should be captured by the fields in Φ_L. Hence we focus our attention on the remaining ten equations. Although slightly fewer in number, solving them is no easy task and will in general require numerical methods. Quite luckily however, some solutions can be found analytically.

4.2.1 Gauge solutions

When imposing the bulk radial gauge, we have not eliminated all gauge freedom in the bulk. Remaining are the "large" gauge transformations which are non-trivial on the boundary, changing what conserved value the Noether current takes. Since the dual field theory lives on the boundary, its physics is affected by these transformations, why they can be used to find *pure gauge* solutions to the fluctuation equations (4.16). The gauge transformations under consideration are the spacetime diffeomorphisms and local $U(1)$ transformations of the Maxwell field:

$$\begin{aligned} g_{\mu\nu} &\to g_{\mu\nu} + \delta_\xi g_{\mu\nu}, \\ A_\mu &\to A_\mu + \delta_\xi A_\mu + \partial_\mu \Lambda, \end{aligned} \tag{4.19}$$

where Λ is the $U(1)$ angle and the vector ξ^μ generates the diffeomorphism, which is given by the Lie derivative as

$$\delta_\xi g_{\mu\nu} = \mathcal{L}_\xi g_{\mu\nu} = \xi^\kappa \partial_\kappa g_{\mu\nu} + g_{\mu\kappa}\partial_\nu \xi^\kappa + g_{\kappa\nu}\partial_\mu \xi^\kappa. \tag{4.20}$$

In order to find the gauge solutions, we make ansätze for the gauge fields consistent with the perturbations as

$$\begin{aligned} \xi^\mu &= \zeta^\mu(r) \mathrm{e}^{-\mathrm{i}\omega t + \mathrm{i}kx + \lambda_2 z}, \\ \Lambda &= \theta(r) \mathrm{e}^{-\mathrm{i}\omega t + \mathrm{i}kx + \lambda_2 z}. \end{aligned} \tag{4.21}$$

$\zeta^\mu(r)$ and $\theta(r)$ can then be solved for by requiring that gauge solutions satisfy the radial gauge condition;

$$\delta_\xi g_{\mu r} = 0 \quad \text{and} \quad \delta_\xi A_r + \partial_r \Lambda = 0. \tag{4.22}$$

The five-component vector ζ^μ and angle θ totals to six independent solutions, determined by six integration constants $c_1, \ldots, c_6$. The linearized equations of motion are invariant under gauge transformations, and the trivial $\Phi = 0$ is a solution, so the pure gauge solutions can be constructed by fixing six linearly independent values of the vector $C = (c_1, \ldots, c_6)$ [21]. The full solutions and their derivations are quite lengthy and can be found in Appendix B.1, but as a representative, consider

$$\delta g_{\mu\nu} = 0, \quad \delta A_\mu = (-\mathrm{i}\omega, \mathrm{i}k, 0, \lambda_2, 0) + \mathcal{O}\Big(r^3\Big) \tag{4.23}$$

obtained by setting $c_6 = 1$ and the remaining constants to zero. Five of the six solutions belong to the longitudinal sector, which means that the number of numerical solutions we need to find are cut in half!

4.2.2 Near-horizon solutions and Frobenius expansions

There is still more work to be done before the remaining solutions to the fluctuation equations can be found, as the fluctuation equations become *singular* at the horizon. This means that part of the equation vanishes in such a way that only the trivial solution remains. To combat this, we employ the method of a *Frobenius expansion*[2] [30]. Consider an ordinary differential equation

$$D(y(x)) = 0 \tag{4.24}$$

where D is a differential operator singular at $x = 0$. With an ansatz $y = x^r\alpha(x)$ where α is analytic, we can series expand $f(x) = \sum_k a_k x^k$ and insert it into (4.24). In the same vein as in Section 2.3, the equation schematically reads as

$$D(y(x)) = I(r)a_0 x^r + \dots \tag{4.25}$$

In order to find a non-trivial solution, a_0 must be non-zero, which leads to the indicial equation $I(r) = 0$. With r specified, x^r can be factored out, whereby $\alpha(x)$ can be solved for.

In our case, this amounts to factoring out a part of the background metric as

$$\delta A_\mu = f(r)^{\mathrm{i}\alpha}\delta A^*_\mu \tag{4.26}$$

and analogously for $\delta g_{\mu\nu}$, where δA^*_μ is the regular field post Frobenius expansion. The pathological behavior near the horizon should now be captured in the factor[3] $f(r)^{\mathrm{i}\alpha}$, since $f(r) \to 0$ as $r \to r_h$. After the removal of this factor, the fluctuation equations (4.16) can be solved for the post-Frobenius fields $\delta g^*_{\mu\nu}$ and δA^*_μ at the horizon. More precisely, we expand the fluctuation equations around the horizon as $r = 1 - \delta$ and solve them to order δ^{-2}, δ^{-1} and δ^0. This way, we find non-trivial solutions to the indicial equation when

$$\alpha = \pm\frac{3\omega}{4(3 - \hat{\mu}^2)}, \quad \text{where} \quad \hat{\mu} < \sqrt{3} \tag{4.27}$$

where we choose the negative sign, corresponding to *infalling boundary conditions*. This can be seen by using the relation between temperature and chemical potential in (4.9);

$$\delta A_\mu = f(r)^{-\mathrm{i}\omega/4\pi T}\delta A^*_\mu \to \mathrm{e}^{-\mathrm{i}\omega\left(t + \frac{1}{4\pi T}\log f(r)\right)}\delta A^*_\mu \tag{4.28}$$

and analogously for $\delta g_{\mu\nu}$, where we restored the explicit time dependence. The negative exponent corresponds to modes that carry energy towards the horizon as $t \to 0$

[2] This works if the singular point is regular. See [30] for more details.

[3] In the literature one often sees $(r_h - r)^{\mathrm{i}\alpha}$ factored out, which is leading behavior of $f(r)^{\mathrm{i}\alpha}$ near the horizon. Factoring out the full $f(r)^{\mathrm{i}\alpha}$ makes the remaining equations slightly prettier.

[17], respecting that information can only flow into the black hole. Computing boundary correlation functions with infalling/outfalling solutions to the bulk equations of motion corresponds to retarded/advanced Green's functions, respectively [17]. In this sense, physically reasonable arguments in the bulk — information cannot escape a black hole — is mirrored in the boundary theory, where the Green's functions should be causal. Note that the gauge solutions in general will not satisfy the infalling boundary conditions. However, they do not generate any flux lines at the horizon, so the singularity is not physical.

Solving the equations at the horizon with infalling boundary conditions also specifies some requirements on the fields themselves; all time-direction components need to be zero, and $\delta g_{xx} + \delta g_{yy} + \delta g_{zz} = 0$ at $r = 1$. We are left with

$$\{\delta A_x, \delta A_y, \delta A_z, \delta g_{xx}, \delta g_{xy}, \delta g_{xz}, \delta g_{yy}, \delta g_{yz}\} \Big|_{r=1} \tag{4.29}$$

as the remaining eight degrees of freedom, five of which live in the longitudinal sector. The full set of fluctuation equation had 28 degrees of freedom, where half are removed by demanding infalling boundary conditions. Combined with the six degrees of freedom $c_1, \ldots, c_6$ from the gauge solutions, all degrees of freedom are now accounted for.

4.2.3 Numerical bulk solutions

Just as for the scalar field in Section 2.3, the fluctuation equations (4.16) can be solved near the boundary. This amounts to making a near-boundary series expansion of δA_μ and $\delta g_{\mu\nu}$, where the corresponding indicial equations implies that

$$\delta A_\mu : \Delta_\pm = 0, 2 \qquad \delta g_{\mu\nu} : \Delta_\pm = 0, 4 \tag{4.30}$$

which means that expansion must contain logarithmic terms, following Section 2.4. At the boundary, we impose that the leading order metric fluctuations vanish; $\delta g^{(0)}_{\mu\nu} = 0$, i.e. that the source for the boundary energy-momentum tensor is zero. Since the factor in front of the logarithmic term is a function of $\delta g^{(0)}_{\mu\nu}$, it is consistent to write the near-boundary expansion of the metric fluctuations as

$$\delta g_{\mu\nu} = \delta g^{(1)}_{\mu\nu} r^4 + \mathcal{O}\Big(r^6\Big). \tag{4.31}$$

On the other hand, we write the near-boundary expansion of the vector field as

$$\delta A_\mu = a^{(0)}_\mu + a^{(1)}_\mu r^2 + B_\mu{}^\nu a^{(0)}_\nu r^2 \log r + \mathcal{O}\Big(r^2\Big), \tag{4.32}$$

where

$$B_\mu{}^\nu \doteq \frac{1}{2}\begin{pmatrix} k^2 - \lambda_2^2 & \omega k & 0 & -\mathrm{i}\omega\lambda_2 \\ -\omega k & -\omega^2 - \lambda_2^2 & 0 & \mathrm{i}k\lambda_2 \\ 0 & 0 & -\omega^2 + k^2 - \lambda_2^2 & 0 \\ \mathrm{i}\omega\lambda_2 & \mathrm{i}k\lambda_2 & 0 & -\omega^2 + k^2 \end{pmatrix} \tag{4.33}$$

is a matrix mixing the different zeroth order components, determined by solving the near-boundary equations to next-to-leading order, in analogy with (2.33). In order to stay in

the grand canonical ensemble with fix chemical potential, the leading order contribution to δA_t needs to vanish at the boundary. However, when solving the fluctuation equations for general values of ω, k and λ_2, $a_t^{(0)}$ may not actually equal zero on the boundary. It is therefore kept it in the above expression for numerical consistency.

These expansions are a good approximation of the true solution when r is small. We may therefore continue by finding the remaining five numerical solutions to the longitudinal fluctuation equations in the region $r \in (\delta, 1-\delta)$, which are given by five different sets of horizon values;

$$\left\{ \Phi_L^{(1)}, \Phi_L^{(2)}, \Phi_L^{(3)}, \Phi_L^{(4)}, \Phi_L^{(5)} \right\} \Big|_{r=1-\delta} \tag{4.34}$$

where each set $\Phi_L^{(i)}$ is defined by setting the ith longitudinal degree of freedom in (4.29) to 1, and the rest to zero.

As discussed, only eight out of the ten fluctuation fields in the longitudinal sector should vanish at the boundary; namely the metric components and the time component of the vector potential. The fact that δA_x and δA_z are not subject to Dirichlet boundary conditions is what models the plasmons [13]. What should be zero at the boundary however, is the specific combination of vector potential components that constitute the plasmon conditions (3.21) and (3.22). We therefore define two auxiliary fields as

$$\begin{aligned} \chi &= \left(\omega^2 + \lambda_2^2\right) \delta A_x + \omega k \delta A_t - \mathrm{i} k \lambda_2 \delta A_z + \mathcal{J}_x / L, \\ \psi &= \left(\omega^2 - k^2\right) \delta A_z - \mathrm{i} k \lambda_2 \delta A_x - \mathrm{i} \omega \lambda_2 \delta A_t + \mathcal{J}_z / L, \end{aligned} \tag{4.35}$$

since $\lim_{r\to 0} L\delta A_i = \mathcal{A}_i$.

Additionally, we wish to satisfy the interface condition (3.14) in order to model surface plasmons. As a neat trick, the fluctuations of the magnetization can be computed by solving the differential equation obtained by taking the derivative of (3.26);

$$\delta M_y' - (\partial_x \delta A_z - \partial_z \delta A_x) = 0. \tag{4.36}$$

This can be added to the list of numerical differential equations. Considering δM_y as an additional fluctuation field to be solved for, the interface condition can be expressed as

$$\mathcal{I}(\omega, k, \lambda_2) = \omega^2 \delta A_x - \sqrt{k^2 - \omega^2} \left(\lambda_2 \delta A_x - \mathrm{i} k \delta A_z - \delta M_y\right), \tag{4.37}$$

which should equal zero on the boundary.

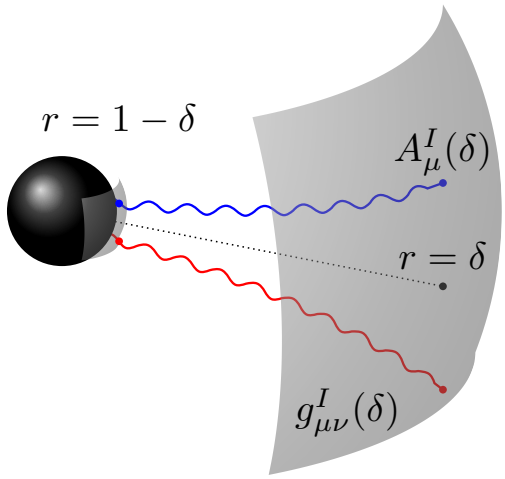

Figure 4.1: Illustration of the numerical problem. Given a set of starting values at the horizon, the corresponding values on the boundary ($r = \delta$) are computed by solving the fluctuation equations in the region $r \in (\delta, 1 - \delta)$.

Consider now a ten-dimensional vector consisting of δA_t and the seven longitudinal fluctuations of the metric together with χ and ψ. There are ten independent solutions to the equations of motion — five pure gauge from Section 4.2.1, and five numerical, defined by the different sets of horizon values in (4.34). At the boundary, numerically situated at $r = \delta$, each field will take on some specific value for each solution. An illustration of this is found in Figure 4.1. The full solution will be a linear combination of the ten independent solutions, specified by constants $C^I, C^{II}, \ldots, C^X$. In matrix form, this can be written as

$$\tilde{\Phi} \equiv \begin{pmatrix} \delta g_{tt}(\delta) \\ \vdots \\ \delta A_t(\delta) \\ \chi(\delta) \\ \psi(\delta) \end{pmatrix}_{\text{tot}} = \begin{pmatrix} \delta g^I_{tt}(\delta) & \cdots & \delta g^X_{tt}(\delta) \\ \vdots & \ddots & \vdots \\ \psi^I(\delta) & \cdots & \psi^X(\delta) \end{pmatrix} \begin{pmatrix} C^I \\ \vdots \\ C^X \end{pmatrix} \equiv \mathcal{X}\mathbf{C} \tag{4.38}$$

where $\delta g^I_{tt}(\delta)$ is the value of δg_{tt} at $r = \delta$ for the first solution, and so on. The boundary conditions demand that the full solution at the boundary, given by the vector $\tilde{\Phi}$, equals the null vector. If we only wish to model bulk plasmons, the interface condition can be ignored, and the existence of a non-trivial solution is the statement that the determinant of the matrix $\mathcal{X}$ in (4.38) vanishes. To additionally investigate if the plasmons are surface plasmons, we compute the eigenvector corresponding to the smallest eigenvalue of the matrix $\mathcal{X}$. This allows for an extraction of the combination of solutions $\mathbf{C}$ that makes $\mathcal{X}$ (numerically) singular, and can be used to check the value of the interface condition (4.37) at the boundary.

4.3 Renormalizing the action

The final hurdle to overcome before the method outlined in the previous section can be implemented, is to properly define the boundary current in terms of the bulk fields, since it appears in the plasmon conditions. This requires us to construct the full action, in analogy to the procedure in Section 2.3 for the scalar field. The theory needs to be properly regulated, and as we saw in (2.24), regulating boundary terms will affect the precise value of the dual boundary operator — in this case the boundary current $\mathcal{J}^\mu$.

Recall the bare Einstein-Maxwell bulk action

$$S_0 = \int_M \mathrm{d}^{d+2}x\sqrt{-g}\,\mathcal{L}_0 = \int_M \mathrm{d}^{d+2}x\sqrt{-g}\left(\frac{R}{2} - \Lambda - \frac{1}{4}F_{\mu\nu}F^{\mu\nu}\right) \tag{4.39}$$

with the negative cosmological constant as required of AdS;

$$\Lambda = -\frac{d(d+1)}{2L^2} \quad = -\frac{6}{L^2} \quad \text{in } \mathrm{AdS}_5 \tag{4.40}$$

In order to have a well-defined variation problem, the Einstein-Hilbert part of the action requires that we add a surface term. The is due to the fact that the Ricci scalar contains second derivatives of the metric field. To see why this is the case, consider

$$\delta\int_M \mathrm{d}^{d+2}x\,\sqrt{-g}\,R = \delta\int_M \mathrm{d}^{d+2}x\,\sqrt{-g}\,\left(R_{\mu\nu} - \frac{1}{2}g_{\mu\nu}R\right)\delta g^{\mu\nu} + \delta\int_M \mathrm{d}^{d+2}x\,\sqrt{-g}\,g^{\mu\nu}\delta R_{\mu\nu} \tag{4.41}$$

where the requirement that the first term vanishes for arbitrary $\delta g^{\mu\nu}$ yields Einstein's equations. Via the Palatini identity, the second term can be re-written as a total covariant derivative. Applying Stokes' generalized theorem then turns this integral into a surface integral over the manifold boundary ∂M;

$$\oint_{\partial M} \mathrm{d}^{d+1}x\,\sqrt{-\gamma}\,n_\mu g^{\mu\nu}g^{\rho\sigma}\left(\delta\partial_\rho g_{\nu\sigma} - \delta\partial_\nu g_{\rho\sigma}\right) \tag{4.42}$$

which normally vanishes when considering open manifolds[4]. To counteract this, we add the *Gibbons-Hawking-York* boundary term, such that the canonical Einstein tensor is obtained from the variation of the Einstein-Hilbert action. The term is [31]

$$S_{\mathrm{GHY}} = \oint_{\partial M} \mathrm{d}^{d+1}x\sqrt{-\gamma}\,K, \qquad K = \gamma^{\mu\nu}\nabla_\mu n_\nu \tag{4.43}$$

where $\gamma_{\mu\nu} \equiv g_{\mu\nu} - n_\mu n_\nu$ is the induced metric on the boundary and K is the trace of the extrinsic curvature of the manifold M. This is a general result, valid for all d, and is needed whenever the manifold has a boundary.

To see what counterterms need to be added, the on-shell action should be investigated. Inserting the background solutions into (4.39), the zeroth-order bare action contributes with

$$S_0^{(0)} = \int_M \mathrm{d}^5x\,\sqrt{g}^{(0)}\mathcal{L}_0^{(0)} = -\int_M \mathrm{d}^5x\left(\frac{4L^3}{r^5} + \mathcal{O}(r)\right) \tag{4.44}$$

[4]For a more detailed calculation, see Appendix B.2.

where we now explicitly study the case at hand with $d = 3$. Integrating out the radial direction up to a cutoff ϵ (i.e. placing ∂M at the finite radius ϵ), we find

$$S_0^{(0)} = -\oint_{\partial M} \mathrm{d}^4x \frac{L^3}{\epsilon^4} + \text{finite}. \tag{4.45}$$

It is interesting to investigate if the Gibbons-Hawking-York boundary term not only makes the variation problem well-defined, but also removes the divergence at the boundary. However,

$$K = -\sqrt{g_{rr}}\gamma^{\mu\nu}\Gamma^r_{\mu\nu} = \frac{1}{2}\gamma^{\mu\nu}n^r\partial_r g_{\mu\nu} = \frac{4}{L} \implies S^{(0)}_{\mathrm{GHY}}\Big|_{r=\epsilon} = \oint_{\partial M} \mathrm{d}^4x \frac{4L^3}{\epsilon^4}. \tag{4.46}$$

We should therefore add a gravitational boundary counterterm

$$S_{\mathrm{ct,\,G}} = -\oint_{\partial M} \mathrm{d}^4x \frac{3L^3}{\epsilon^4} \tag{4.47}$$

in agreement with [32].

The above calculations can now be repeated for the first-order action $S^{(1)}$. The first-order Lagrangian contributes with

$$\mathcal{L}_0^{(1)} = \frac{2r^4}{L^2}\eta^{\mu\nu}\delta g^{(1)}_{\mu\nu} + \mathcal{O}\Big(r^6\Big) \tag{4.48}$$

neglecting the plane wave factor, with the $\delta g_{\mu\nu}$ as defined in (4.12), i.e. with L^2/r^2 already factored out. This might seem troublesome since it seems to lead to a logarithmic divergence on the boundary, but the fluctuations in $\sqrt{-g}$ need to be accounted for. Writing the metric as

$$g_{\mu\nu} = \mathfrak{g}_{\mu\nu} + \epsilon h_{\mu\nu} \tag{4.49}$$

where $\mathfrak{g}_{\mu\nu}$ is the background metric and $h_{\mu\nu}$ are the perturbations, the square root of the metric reads

$$\begin{aligned}\sqrt{-\det(\mathfrak{g}+\epsilon h)} &= \sqrt{-\det\mathfrak{g}}\sqrt{\exp\Big\{\mathrm{Tr}\Big\{\log\left(1+\epsilon\mathfrak{g}^{-1}h\right)\Big\}\Big\}} \\ &= \sqrt{-\det\mathfrak{g}}\left(1+\frac{\epsilon}{2}\,\mathrm{Tr}\Big\{\mathfrak{g}^{-1}h\Big\}\right) + \mathcal{O}\Big(\epsilon^2\Big) \implies \\ \Big(\sqrt{-g}\Big)^{(1)} &= \frac{L^5}{2r}\eta^{\mu\nu}\delta g^{(1)}_{\mu\nu} + \mathcal{O}(1)\end{aligned} \tag{4.50}$$

up to plane wave factors, using the near-boundary expansion of the metric fluctuations (4.31) and that $f(r)^{-1} = 1 + \mathcal{O}(r)$. Taken all together, this means that

$$\begin{aligned}S_0^{(1)} &= \int_M \mathrm{d}^5x \left(\sqrt{-g}^{(0)}\,\mathcal{L}_0^{(1)} + \sqrt{-g}^{(1)}\,\mathcal{L}_0^{(0)}\right) \\ &= \int_M \mathrm{d}^5x \left(\frac{L^5}{r^5}\frac{2r^4}{L^2} - \frac{L^5}{2r}\frac{4}{L^2}\right)\eta^{\mu\nu}\delta g^{(1)}_{\mu\nu} + \mathcal{O}(1) = \int_M \mathrm{d}^5x\,\mathcal{O}(1)\end{aligned} \tag{4.51}$$

which is finite. The Gibbons-Hawking term will also contributes to first order in ϵ due to the factor of $\partial_r g_{\mu\nu}$ in K; up to plane wave factors,

$$S^{(1)}_{\mathrm{GHY}} = \oint_{\partial M} \mathrm{d}^4x\, L^3\eta^{\mu\nu}\delta g^{(1)}_{\mu\nu} \tag{4.52}$$

which also is finite.

4.3.1 Second order action and Maxwell counterterms

Extending the calculation in (4.50) to second order will necessarily include two factors of $\delta g_{\mu\nu} \sim r^4$, so $\sqrt{-g}^{(2)} \sim r^3$. This means that both terms $\sqrt{-g}^{(1)}\mathcal{L}_0^{(1)} \sim \sqrt{-g}^{(2)}\mathcal{L}_0^{(0)} \sim r^3$ are convergent, so we focus our attention to the expansion of the Lagrangian to second order. Furthermore, the Einstein-Hilbert part is convergent, so consider the Maxwell part of the bare action

$$S_{0,\mathrm{M}} = -\frac{1}{4}\int_M \mathrm{d}^5x\sqrt{-g}\,F_{\mu\nu}F^{\mu\nu} = -\frac{1}{2}\int_M \mathrm{d}^5x\sqrt{-g}\,\nabla_\mu A_\nu F^{\mu\nu}. \tag{4.53}$$

Using Stokes' to integrate by parts,

$$S^*_{0,\mathrm{M}} = -\frac{1}{2}\oint_{\partial M} \mathrm{d}^4x\sqrt{-\gamma}\,n_\mu A_\nu F^{\mu\nu} \tag{4.54}$$

where the bulk term contains the equations of motion $\nabla_\mu F^{\mu\nu}$ and thus vanishes on-shell. With the near-boundary expansion of the vector field in (4.32), the action reads

$$\begin{aligned} S^*_{0,\mathrm{M}} &= \frac{L}{2}\oint_{\partial M} \mathrm{d}^4x\frac{1}{r}A_\nu\eta^{\mu\nu}\partial_r A_\mu \implies \\ \left(S^*_{0,\mathrm{M}}\right)^{(2)} &= \frac{L^3}{2}\oint_{\partial M} \mathrm{d}^4x\,\eta^{\mu\nu}\left(2a^{(0)}_\mu a^{(1)}_\nu + a^{(0)}_\mu B_\nu{}^\kappa a^{(0)}_\kappa + 2a^{(0)}_\mu B_\nu{}^\kappa a^{(0)}_\kappa \log r\right) + \mathcal{O}(r) \end{aligned} \tag{4.55}$$

where we used the unit normal $n_r = -L/r$ and that $F^{r\nu} = g^{rr}\gamma^{\mu\nu}\partial_r A_\mu$ in radial gauge. The transseries expansion of the vector field is therefore responsible for the divergent logarithm as $\epsilon \to 0$, which needs to be regulated. We add the counterterm

$$S_{\mathrm{ct}} = L\log(r)\oint_{\partial M} \mathrm{d}^4x\sqrt{-\gamma}\,\frac{1}{4}F_{\mu\nu}F^{\mu\nu} \tag{4.56}$$

since

$$\oint_{\partial M} \mathrm{d}^4x\sqrt{-\gamma}\,F_{\mu\nu}F^{\mu\nu} = 2\oint_{\partial M} \mathrm{d}^4x\,\nabla_\mu\left(\sqrt{-\gamma}\,A_\nu\right)F^{\mu\nu} = -2\oint_{\partial M} \mathrm{d}^4x\sqrt{-\gamma}\,A_\nu\partial_\mu F^{\mu\nu} \tag{4.57}$$

where we have used that the metric is covariantly constant, integrated by parts, that $\partial(\partial M) = 0$ and $\nabla_\mu F^{\mu\nu} = \partial_\mu F^{\mu\nu}$[5]. In terms of the fluctuations, the counterterm action takes on the value

$$S^{(2)}_{\mathrm{ct}} = \frac{1}{2}L^3\log(r)\oint_{\partial M} \mathrm{d}^4x\sqrt{-\gamma}\,\delta A_\nu\partial_\mu\eta^{\mu\rho}\eta^{\nu\sigma}\left(\partial_\rho\delta A_\sigma - \partial_\sigma\delta A_\rho\right). \tag{4.58}$$

Since the indices run over boundary coordinates, it is clear from (4.32) that any terms containing $\log r$ come with additional factors of r^2. As such, to lowest order in r, only the leading order coefficients $a^{(0)}_\mu$ contribute, such that

$$S^{(2)}_{\mathrm{ct}} = L^3\log(r)\oint_{\partial M} \mathrm{d}^4x\left[a^{(0)}_\nu\partial_\mu\eta^{\mu\rho}\eta^{\nu\sigma}\partial_{[\rho}a^{(0)}_{\sigma]} + \mathcal{O}(r)\right], \tag{4.59}$$

precisely canceling the divergent term in (4.55). The action is now finite to second order, which means that the boundary operator $\mathcal{J}^\mu$ has been renormalized.

[5]The term $\Gamma^\nu_{\mu\kappa}F^{\mu\kappa} = 0$ from the opposite symmetry in μ and κ. $\Gamma^\mu_{\mu\kappa}F^{\kappa\nu} = 0$ since the metric is diagonal.

4.3.2 Definition of the current

Since S_{ct} is a function of A_μ, it will contribute to the boundary current. But from (4.59) it should be clear that the only addition to the current is the one to cancel the logarithmic term in (4.55). Note however that the transseries is also responsible for a factor $B_\mu{}^\nu a_\nu^{(0)}$ that shows up without a logarithm in (4.55), which therefore will contribute to the current, schematically as $\mathcal{J} \sim 2a^{(1)} + Ba^{(0)}$. We therefore make the choice to add yet another boundary term, not to cancel any divergences, but to *make the current canonical*, i.e. identified with the sub-leading term in the near-boundary expansion as $\mathcal{J} \sim 2a^{(1)}$. From the calculations above, and the structure of the terms in (4.55), it is clear that this is achieved by the term

$$S_{\text{FF}} = \frac{L}{2} \oint_{\partial M} \mathrm{d}^4x \sqrt{-\gamma}\, F_{\mu\nu} F^{\mu\nu} \tag{4.60}$$

as this will, to lowest order in r, precisely cancel the term $\eta^{\mu\nu} B_\mu{}^\nu a_\nu^{(0)}$ in (4.55).

This sleight of hand requires some justification, so consider a rescaling of the vector field by a factor $\sqrt{\lambda}$ such that the boundary vector potential is identified as

$$\lim_{r\to 0} A_\mu/\sqrt{\lambda} = \mathcal{A}_\mu. \tag{4.61}$$

In the boundary theory, the $\mathcal{J}^\mu \mathcal{A}_\mu$ has to be left invariant — $\mathcal{J}^\mu$ and $\mathcal{A}_\mu$ are conjugate operators, related to each other via a Legendre transform, and we wish that (2.10) holds with no additional factors of λ. This is solved by identifying $\mathcal{J}^\mu \sim \sqrt{\lambda} 2a^{(1)}$, which leaves the boundary physics unchanged. However, this means that the bulk electromagnetic field tensor will go from

$$\frac{1}{4e^2} F_{\mu\nu} F^{\mu\nu} \to \frac{1}{4e^2\lambda} F_{\mu\nu} F^{\mu\nu} \tag{4.62}$$

as seen from the boundary, where we have explicitly written out the factors of e[6]. Hence, λ can be identified as a constant relating the strength of electromagnetic interactions on the boundary ($\sim e$) and in the bulk ($\sim \sqrt{\lambda} e$). The additional boundary term added to make the current canonical then simply leads to a simple rescaling

$$\frac{1}{\lambda} \to \frac{1}{\lambda} - \frac{1}{2}. \tag{4.63}$$

For reasonable values of λ (i.e. not $\lambda = 0$, for instance), boundary physics should be unchanged, given proper redefinitions of the boundary operators. We therefore argue that the effect of shifting λ by some small amount should not a problem, although the case $\lambda = 2$ should probably be investigated more thoroughly in the future.

To conclude, the full action is given by

$$S = S_0 + S_{\text{GHY}} + S_{\text{ct, G}} + S_{\text{ct}} + S_{\text{FF}} \tag{4.64}$$

which on-shell reads

$$S^* = L^3 \oint_{\partial M} \mathrm{d}^4x\, \eta^{\mu\nu} 2a_\mu^{(0)} a_\nu^{(1)} + \dots \tag{4.65}$$

[6]This factor can always be hidden by a redefinition of the fields.

such that the boundary current is obtained as

$$\langle \mathcal{J}^\mu \rangle = \frac{\delta S^*}{\delta A_\mu} = 2L^2 a_\nu^{(1)} \eta^{\mu\nu}. \tag{4.66}$$

With a proper deviation of the current, the plasmon conditions can be expressed purely in terms of the bulk fields as

$$\begin{aligned} \chi &= \left(\omega k \delta A_t + (\omega^2 + \lambda_2^2)\delta A_x - \mathrm{i} k \lambda_2 \delta A_z\right)\left(\frac{3}{2} + \log r\right) + \frac{\delta A_x'}{r} \\ \psi &= \left(-\mathrm{i}\omega\lambda_2 \delta A_t - \mathrm{i} k \lambda_2 \delta A_x + (\omega^2 - k^2)\delta A_z\right)\left(\frac{3}{2} + \log r\right) + \frac{\delta A_z'}{r}. \end{aligned} \tag{4.67}$$

This takes care of the fact that $\mathcal{J}_i \neq \delta A_i'/r$ due to the logarithmic divergence.

4.4 Numerical implementation

It is time to assemble the computational machinery described in this chapter. First, we choose a ratio between the boundary chemical potential and temperature, specifying the grand canonical ensemble. The given value of μ/T defines the static background solution (4.8), around which the perturbations defined in (4.12) and (4.13) may be solved for.

Given specific values of the parameters ω, k and λ_2, we compute five different solutions to the fluctuations equations in the region from near the horizon, $r = 1 - \delta$, to near the boundary, $r = \delta$, in Mathematica using `NDSolve`, following Section 4.2.3. Numerically, δ has to be small enough, and we have determined that

$$\delta = 10^{-5} \tag{4.68}$$

produces stable solutions. Combined with the analytical gauge solutions in Section 4.2.1, the matrix $\mathcal{X}$ in (4.38) may then be constructed. To determine the dispersion relation, we search the parameter space spanned ω, k and λ_2 for values where where the determinant of $\mathcal{X}$ is (numerically) zero. In the regions where this conditions is met, the boundary conditions are satisfied, i.e. that:

1. the fluctuations of the metric components vanish, ensuring that there is no dynamical graviton on the boundary,
2. the fluctuations of the time component of the vector potential vanishes, ensuring that the background is at a static chemical potential,
3. the auxiliary fields χ and ψ vanish, ensuring that the plasmon condition is satisfied on the boundary.

Additionally, the search can be restricted to surface plasmons, by searching for values where the interface condition $\mathcal{I}$ is (numerically) zero as well.

The explicit dispersion relation can then be obtained by tracking a mode (a solution to the above requirements) through the space spanned by ω, k, λ_2 and μ. In general, both

$\det \mathcal{X}$ and $\mathcal{I}$ will take on complex values, so an eloquent way to implement that condition that both are numerically zero, is to consider the simultaneous optimization problems

$$\min_{\omega,k,\lambda_2\in\mathbb{C}} \log\left|\det \mathcal{X}(\omega,k,\lambda_2)\right| \quad \text{and} \quad \min_{\omega,k,\lambda_2\in\mathbb{C}} \log\left|\mathcal{I}(\omega,k,\lambda_2)\right|. \tag{4.69}$$

Here, one of ω and k can be restricted to being real, following our discussion in Section 3.1. Additionally, with the direction of propagation in the positive x-direction, we may without loss of generality demand that $\operatorname{Re} k \geq 0$. The optimization space is also restricted by physical reasons to

$$\operatorname{Re}\omega \geq 0, \quad \operatorname{Im}\omega < 0, \quad \operatorname{Im} k > 0 \quad \operatorname{Re}\lambda_2 \geq 0 \tag{4.70}$$

as the latter three otherwise would correspond to exponentially growing solutions.

The functions to be minimized in (4.69) are implemented as a Mathematica function. This is latter called upon in Python via the *Wolfram Client library for Python* [33]. The mode tracking algorithm is as follows:

1. Consider one of the parameters μ/T, k or ω to be fix, and choose another, call it x, through which the dispersion relation will be tracked.
2. At some value of x, minimize the cost function.
3. Based on the position of the found minima, update the optimization area for the next value of x based on the previous positions, by extrapolating the value of the derivative in x-space.

At each point, the cost function is minimized using a Bayesian optimization procedure, implemented through the package `skopt` [34]. As the cost function is a "black box", in addition to being relatively costly to compute, Bayesian optimization is a solid choice, as it does not rely on computations of the gradient or Hessian. In short, the particular method implemented relies on Gaussian processes in order to make an informed decision about where to sample the objective function next.

5. Results

This chapter highlights the numerical results obtained from the performed simulations. First, bulk plasmons in three dimensions are investigated. As this has not been done before, these new results are compared with previous results, which serves as a valuable validation of the model, before embarking on the quest to find the surface plasmon polartion dispersion.

5.1 Bulk plasmons in three dimensions

Holographic bulk plasmons in two dimensions have been studied previously using an AdS_4 Reissner-Nordström model [13], [15], arguing that the bulk plasmon properties are qualitatively the same in two and three dimensions. Working in two spatial dimensions simplifies the calculations greatly, and avoids the problem of the logarithmic divergence of the fields near the boundary. Extending this to an AdS_5 model with three spatial dimensions on the boundary serves two purposes. Firstly, it investigates the validity of the argument in the above papers. Secondly, and most importantly, it serves as a cross-validation for the AdS_5 model constructed in Chapter 4, especially with regards to the choice of the added S_{FF} counterterm which makes the current canonical.

In order to model bulk plasmons, the attenuation parameter λ_2 should be set to zero, and the interface condition should be ignored. This means that the z-components of the fluctuation fields decouple in the fluctuation equations, why the calculations can be restricted to the seven components

$$\Phi_{BP} = \left\{\delta g_{tt}, \delta g_{tx}, \delta g_{xx}, \delta g_{yy}, \delta g_{zz}, \delta A_t, \delta A_x\right\}. \tag{5.1}$$

Since there are four gauge solutions in this sector, the number of numerical solutions are reduced to three, speeding up the calculations. Additionally, the plasmon condition in the z-direction can be ignored, so the combination of solutions now reads

$$\begin{pmatrix} \delta g_{tt}(\delta) \\ \vdots \\ \delta A_t(\delta) \\ \chi(\delta) \end{pmatrix}_{\text{tot}} = \begin{pmatrix} \delta g^I_{tt}(\delta) & \cdots & \delta g^{VII}_{tt}(\delta) \\ \vdots & \ddots & \vdots \\ \chi^I(\delta) & \cdots & \chi^{VII}(\delta) \end{pmatrix} \begin{pmatrix} C^I \\ \vdots \\ C^{VI} \end{pmatrix} \equiv \tilde{\mathcal{X}}\tilde{C} \tag{5.2}$$

where the determinant of the above seven-by-seven matrix $\tilde{\mathcal{X}}$ is used to find the modes. In the following, we let k be real, such that the decay is modeled by $\operatorname{Im}\omega$, allowing us to speak of the modes being "long-lived" or not.

The system is studied in a handful of different regimes; where $\mu/T = \{0, 1, 5, 10\}$. The first corresponds to incompressible matter, which is not a common state of matter in the real world, although it can be created in a laboratory by tuning certain systems to their critical points [9]. However, it serves as a theoretically interesting limit, and can furthermore be used to compare the model to theoretical predictions valid in this regime. Gran et al. found "exotic" plasmon dispersion relations for an AdS_4 model in the region $0 < \mu/T \lesssim 2$ [15]. Hence $\mu/T = 1$ allows for an illustration of some of these abnormal features, as well as being an interesting intermediate scale not easily accessible by non-holographic methods. Lastly, $\mu/T = 5$, 10 is chosen to represent the system when the charge density effects dominate, as when μ/T is large, the model approaches that of zero-temperature, finite density matter. In this regime, the system should behave more like a normal metal, as an abundance of charge should lead to screening effects, weakening the coupling.

Before starting the mode tracking procedure outlined in Section 4.4, we first perform a sweep in $\omega \in \mathbb{C}$, for some fixed, small value of the wave vector $\hat{k}$. This allows for an easy access to starting points for the optimizer, and gives a good visual representation of the existing modes. Figure 5.1 shows the logarithm of the determinant of the matrix in (5.2) for different values of μ/T. Hence, dark regions in the heatmaps indicate where the determinant is close to zero, i.e. the existence of plasmon modes. Bright regions corresponds to a diverging determinant, and occur at points where the differential equations become singular. Note that for $\mu/T = 0$, a slightly larger wave vector is chosen for visibility, as this pushes the modes further from the origin.

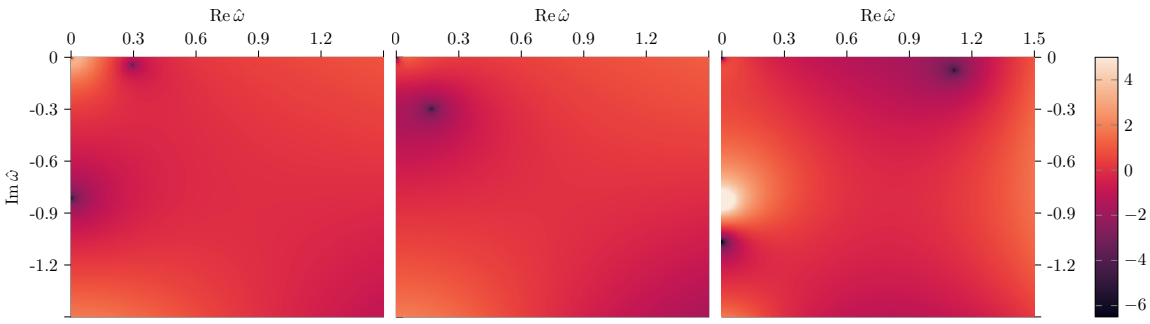

a) $\mu/T = 0$ **b)** $\mu/T = 1$ **c)** $\mu/T = 10$

Figure 5.1: Parametric sweep of $\log|\det\{\tilde{\mathcal{X}}\}|$ with $\tilde{\mathcal{X}}$ as in (5.2), for $\mu/T = 0$ with $\hat{k} = 0.5$, and $\mu/T = 1$, 10 with $\hat{k} = 0.1$. Dark regions indicate the existence of plasmon modes.

In order to make the modes more visible, the plots have been normalized in two ways. Before the logarithm is taken, the error is first divided by the sum of the parameters squared[1], since a fix relative error implies a larger absolute error further away from the origin in the parameter space. This also partly removes the fake mode at k, $\omega = 0$, which

[1]The fluctuation equations depend quadratically on the parameters, see e.g. (4.17).

is a trivial solution. Additionally, a parabolic fit is made to the logarithm of the error in the entire sweep region. This background is then subtracted, making the essential features more prominent.

In the heatmaps for $\mu/T = 0$ and $\mu/T = 10$, two types of modes are visible: purely diffusive modes located along the imaginary axis, and long-lived, propagating modes with respectable real part. Interestingly, in the intermediate region, where $\mu/T = 1$, the diffusive mode seems to have disappeared, and the remaining mode has acquired significant damping. We will return to the discussion of this mode shortly.

The locations of the modes shown in Figure 5.1 can now serve as starting points for the optimization algorithm described in Section 4.4, allowing them to be tracked through $\hat{k}$-space. The dispersion relations for the propagating modes are shown in Figure 5.2, and are in good agreement with those found by Gran et al. [13], [15] in two spatial dimensions.

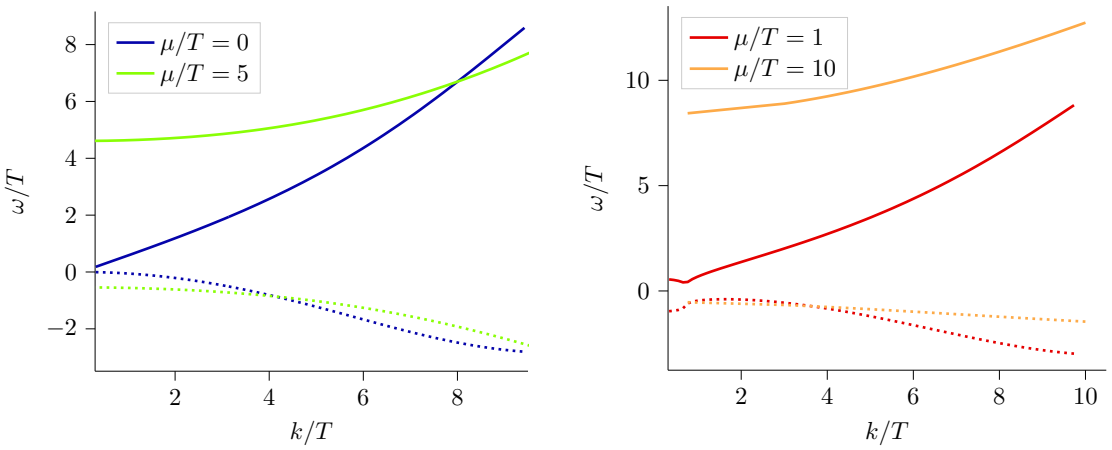

Figure 5.2: Sound modes of the bulk plasmon system for various values of the boundary chemical potential. Real and imaginary parts are shown as solid and dotted lines, respectively.

When the chemical potential is zero, there is no source for the charge density fluctuations. Hence the modes all have $\mathcal{A}_\mu = 0$, i.e. they are purely gravitational, from the bulk point of view. The propagating mode for $\mu = 0$ is therefore not related to the propagation of plasmons of the system, but can be seen as a fundamental feature of "quantum sound" for the system [9]. Recall that the bulk metric is dual to the boundary energy-momentum tensor $T^{\mu\nu}$. Even though the fluctuations vanish on the boundary, the existence of a mode with non-trivial $\delta g_{\mu\nu}$ in the bulk, can be interpreted as fluctuations of the boundary $T^{\mu\nu}$ in the IR, or more concretely, density waves, as T^{ij} represents momentum flux.

In this regime of zero-density, finite-temperature physics i, the "thermal fluid" can be modeled by Navier-Stokes-like hydrodynamics [9], valid in the regime where k/T is small.

This tells of a longitudinal sound mode with the dispersion

$$\omega = \pm v_s k - \mathrm{i}\Gamma_s k^2 \tag{5.3}$$

where Γ_s is an attenuation constant and $v_s = 1/\sqrt{d}$ is the "speed of zero sound" [9]. This theoretical prediction is in good agreement with our results, where a numerical fit in the region near the origin agrees with $v_s = 1/\sqrt{3} \approx 0.58$ to two decimal points.

When $\mu/T = 1$, there is a kink in the dispersion curve at $k/T \approx 0.5$. This is the exotic behavior illustrated in [15], where the collision of modes forms new propagating modes with anomalous behavior. This is a true plasmon mode, with a characteristic "gap" due to the non-zero chemical potential. The gapped behavior is even more prominent for the sound modes at $\mu/T = 5$, 10, where the gap is roughly proportional to the size of μ/T.

We conclude that the holographic framework seems to work as expected when extended to three space dimensions on the boundary. The results support the choice of the addition of the boundary term S_{FF} in (4.60), making the current canonical, although the effect of a a non-canonical current relation would have to be explored before drawing any definite conclusions. The existence of exotic behavior at certain values of μ/T seems to persist in three dimensions, which bodes well for the prospect of finding unique dispersion relations for surface plasmons, as this exoticism is only accessible through holographic models [15].

5.2 Surface plasmon polaritons

On the back of the results presented in the previous section, we are now ready to move on to the uncharted waters of strongly coupled surface plasmon polaritons using holography. When considering surface plasmons, it is convenient to let k be complex instead of ω. A surface plasmon polariton travels some finite distance along the interface, why it makes more sense to consider the decay in space as opposed to time. Furthermore, it elucidates the comparison to the decay into the dielectric, λ_2, and relates well to an experimental setting, since a laser with tuneable imaginary frequencies has not been invented yet.

The problem is quite a bit more intricate than in the bulk plasmon case, as a sweep of the entire two-dimensional complex space spanned by k and λ_2 cannot be visualized easily, in addition to being very costly to compute. Although far from perfect as a means of visualizing the location of a mode, Figure 5.3 shows a sweep in $\mathrm{Re}\,\hat{k}$ and $\mathrm{Re}\,\hat{\lambda_2}$ for $\hat{\omega} = 0.1$ and $\mu/T = 1/3$, where $\mathrm{Im}\,\hat{k} = 0.007$ is based on the position of the corresponding bulk plasmon mode, and $\mathrm{Im}\,\hat{\lambda_2} = 0$.

The k in the bulk plasmon dispersion shown in Figure 5.2 is the full wavevector, and assumes that the setup is isotropic, such that the x-axis can be aligned along the direction of propagation, without loss of generality. Inverting the dispersion in (5.3), which should

be a good approximation for k, ω and μ small, tells us that

$$\hat{k} \approx 0.17 + 0.08\mathrm{i} \quad \text{when} \quad \hat{\omega} = 0.1, \tag{5.4}$$

which agrees with the asymptotic behavior in Figure 5.3a as λ_2 approaches zero. The problem is that the SPP setup does not have the same symmetry, as the wave vector $\boldsymbol{k} = (k, 0, \mathrm{i}\lambda_2)$ cannot be rotated to lie along only one axis. Hence larger values of λ_2 implies an anisotropy not captured by the bulk plasmon dispersion, why it cannot be used to reduce the dimensionality of the optimization problem by scanning the interface condition along the dark region in Figure 5.3a, where $\det|\mathcal{X}|$ is close to zero. However, we note that this region roughly follows the curve where real part of the full wave vector, which can be approximated by $\sqrt{(\mathrm{Re}\, k)^2 - (\mathrm{Re}\, \lambda_2)^2}$ when the other parameters are small, is constant and equal to the value predicted by (5.4).

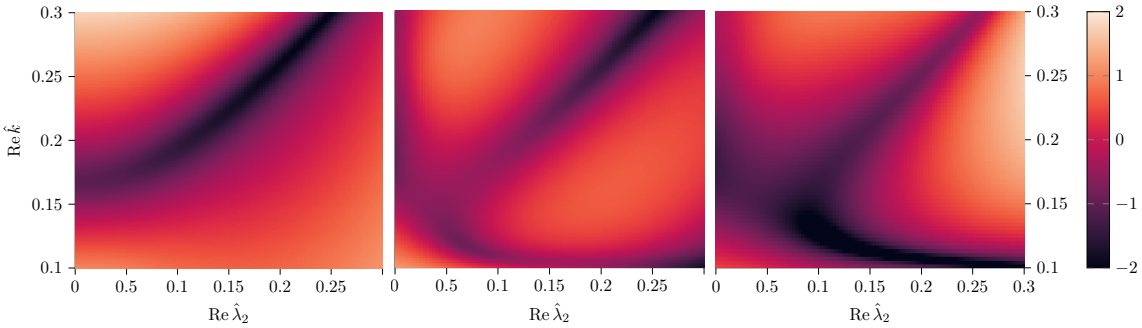

a) $\log|\det \mathcal{X}|$ **b)** $\mathcal{I}(\omega, k, \lambda_2)$ **c)** $\mathcal{I}(\omega, k, \lambda_2)$, $\mathcal{M}_y = 0$

Figure 5.3: Parametric sweep in the Re $\hat{k}$-Re $\hat{\lambda_2}$ plane with Im $\hat{k} = 0.007$ and Im $\hat{\lambda_2} = 0$, for $\hat{\omega} = 0.1$ and $\mu/T = 1/3$. The effect of removing the magnetization from the interface condition is shown in c).

The corresponding sweep for the interface condition is shown in Figure 5.3b. This features a region with the same asymptotic behavior as in the sweep for $\det|\mathcal{X}|$. Although they gradually overlap as one moves away from the origin, it produces no well-defined minimum. However, we can also glimpse a $1/x$-shaped region, why it might exist a common minimum at the intersection of this region with the one in Figure 5.3a. Sadly, the optimizer is unable to find a well-defined local minimum.

The problem can partly be attributed to the effect of the magnetization. Figure 5.3c shows the effect of neglecting $\mathcal{M}_y$ in the interface condition. Although the main region that is impacted, near the bottom of Figure 5.3c, is not physical (this it not a minimum for the remaining boundary conditions), there is a noticeable change along the line in Figure 5.3a as well. This supports the assumption that the fluctuations in the magnetization should not be neglected, at least not in the regime where μ/T is small. This might be a hint of something "exotic", akin to the kink in Figure 5.2, captured by non-negligible magnetic effects.

However, this presents an opportunity to study an easier subproblem, by assuming that the magnetization is zero, i.e. making some assumptions on the strange metal. We can then follow the standard plasmon literature and assume that the magnetic field inside of the metal satisfies a simple wave equation [24], which leads to the relation

$$\lambda_2^2 = k^2 - \omega^2 \varepsilon_2. \tag{5.5}$$

Combined with the continuity of $\mathcal{E}_x$ at the interface, λ_2 can be solved for, as

$$\frac{\lambda_1}{\lambda_2} = -\frac{\varepsilon_1}{\varepsilon_2} \quad \Longrightarrow \quad \lambda_2 = \frac{k^2}{\sqrt{k^2 - \omega^2}}, \tag{5.6}$$

which allows for a reduction in dimensionality of the optimization problem. Additionally, the interface condition is always satisfied, so we only need to study the value of the determinant. Choosing a relatively large value of μ/T should allow the system to behave more as expected classically, according to the results in Figure 5.2. Following the procedure in the previous section, we find one interesting dispersion relation, shown in Figure 5.4. This does not exhibit the typical behavior of a surface plasmon polariton dispersion curve, where $k(\omega)$ has the shape of an "S" [24], but it captures *some* feature, in the small kink around $\omega/T \approx 4.5$.

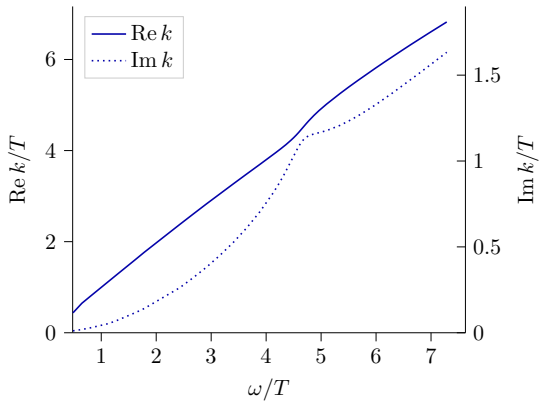

Figure 5.4: SPP dispersion relation for $\mu/T = 5$, assuming no magnetization.

6. Conclusion and Outlook

The extension of the relatively well-established AdS_4 Reissner-Nordström metal to the less common AdS_5 version poses several difficulties. However, since the results for the bulk plasmons are in good agreement with previous results, it seems that the extension in dimensionality can be done by adequately treating the divergent logarithmic terms.

A more complete treatment of bulk plasmons in three spatial dimensions could address a couple of shortcomings of this thesis. These include expanding the search space in order to find additional, higher order modes, and to investigate the transverse sector for completeness. The latter should be low-hanging fruit since the procedure is essentially the same, but with fewer fields to solve for. Finally, the region with exotic dispersion could be investigated more thoroughly, to see if there are any dimension-dependent behavior. Based on our findings, it is however likely that the two-dimensional results in [13], [15] generalize to three dimensions as expected.

The interest in increasing the number of dimensions mostly pertains to the study of holographic surface plasmons. The quest of finding a point in the parameter space which satisfies all boundary conditions proves to be a difficult task, but the possibility of finding such a point should not be ruled out. As this problem has not been studied before, it is possible that there is some error in the analysis. Alternatively, a more sophisticated optimization method must be used, which for instance can address the problem of weighing both the plasmon and interface conditions equally. One such workaround is to group the interface condition with the rest of the fields in the matrix equation in (4.38), and search for the null vector to the resulting 10-by-11 matrix. However, although this might make the optimization easier, it makes the search for an initial mode to track very difficult, since the parameter space is so large.

Another plausible, but computationally costly, method is to determine the anisotropic bulk plasmon dispersion relation for various values of λ_2. With a relation between the full wavevector $\boldsymbol{k} = (k, 0, \mathrm{i}\lambda_2)$ and the frequency ω, the interface condition can be optimized under the constraint that the parameters satisfy the plasmon conditions.

Although the problem can be simplified by following the steps around (5.6), it is probably a good idea not to make too many assumptions when dealing with physics for which we have limited intuition. Magnetic effects are usually suppressed, but when the coupling is strong, we really do not know what to expect. Figure 5.3c clearly shows that the effect of

the fluctuations in magnetization is highly relevant, at least when μ/T is small. However, it might be worthwhile to study the surface plasmon dispersion shown in Figure 5.4 in more detail, for various values of μ/T. An understanding of how this dispersion behaves for different parameter values could then serve as a valuable reference for when the simplification in (5.6) is relaxed. As the full picture seems to require the inclusion of the magnetization, transverse electric (TE) modes should be studied as well, since they are supported when $\mu < 0$ [25].

Finally, the effects of a material with non-zero equilibrium magnetization can be implemented by extending the background Reissner-Nordström solution to that of a *dyonic black brane* [35]. This would add an additional parameter defining the magnetic charge of the brane, related to the value around which the magnetization would be allowed to fluctuate.

In conclusion, magnetic effects seems to be important for surface plasmon polaritons in strange metals, in contrast to the normal analysis in a weakly coupled regime. A holographic approach can produce a model that incorporates such strongly correlated behavior, but more work is needed in order to obtain a complete dispersion relation.

References

[1] T. Aoyama, M. Hayakawa, T. Kinoshita, and M. Nio, "Tenth-Order QED Contribution to the Electron g-2 and an Improved Value of the Fine Structure Constant," *Phys. Rev. Lett.*, vol. 109, no. 11, 111807, p. 111 807, 2012-09. DOI: 10.1103/PhysRevLett.109.111807. arXiv: 1205.5368 [hep-ph].

[2] F. J. Dyson, "Divergence of perturbation theory in quantum electrodynamics," *Phys. Rev.*, vol. 85, pp. 631–632, 4 1952-02. DOI: 10.1103/PhysRev.85.631.

[3] A. Legros, S. Benhabib, W. Tabis, *et al.*, "Universal T-linear resistivity and Planckian dissipation in overdoped cuprates," *Nature Physics*, vol. 15, no. 2, pp. 142–147, 2019-02. DOI: 10.1038/s41567-018-0334-2.

[4] Y. Cao, D. Chowdhury, D. Rodan-Legrain, *et al.*, "Strange Metal in Magic-Angle Graphene with near Planckian Dissipation," *Phys. Rev. Lett.*, vol. 124, p. 076 801, 7 2020-02. DOI: 10.1103/PhysRevLett.124.076801.

[5] S.-D. Chen, M. Hashimoto, Y. He, *et al.*, "Incoherent strange metal sharply bounded by a critical doping in Bi2212," *Science*, vol. 366, no. 6469, pp. 1099–1102, 2019. DOI: 10.1126/science.aaw8850.

[6] J. Maldacena, "The Large-N Limit of Superconformal Field Theories and Supergravity," *International Journal of Theoretical Physics*, vol. 38, no. 4, pp. 1113–1133, 1999-04. DOI: 10.1023/A:1026654312961.

[7] S. W. Hawking, "Particle creation by black holes," *Communications in Mathematical Physics*, vol. 43, no. 3, pp. 199–220, 1975-08. DOI: 10.1007/BF02345020.

[8] H. Fritzsch, "Fundamental Constants at High Energy," *Fortschritte der Physik*, vol. 50, no. 5-7, pp. 518–524, 2002-05. DOI: 10.1002/1521-3978(200205)50:5/7<518::aid-prop518>3.0.co;2-f.

[9] J. Zaanen, Y.-W. Sun, Y. Liu, and K. Schalm, *Holographic Duality in Condensed Matter Physics*. Cambridge University Press, 2015.

[10] D. Pines and D. Bohm, "A Collective Description of Electron Interactions: II. Collective vs Individual Particle Aspects of the Interactions," *Phys. Rev.*, vol. 85, pp. 338–353, 2 1952. DOI: 10.1103/PhysRev.85.338.

[11] C. Langhammer, I. Zorić, B. Kasemo, and B. M. Clemens, "Hydrogen Storage in Pd Nanodisks Characterized with a Novel Nanoplasmonic Sensing Scheme," *Nano Letters*, vol. 7, no. 10, pp. 3122–3127, 2007-10. DOI: 10.1021/nl071664a.

[12] M. Mitrano, A. A. Husain, S. Vig, *et al.*, "Anomalous density fluctuations in a strange metal," *Proceedings of the National Academy of Sciences*, vol. 115, no. 21, p. 5392, 2018-05. DOI: 10.1073/pnas.1721495115.

[13] U. Gran, M. Tornsö, and T. Zingg, "Holographic plasmons," *Journal of High Energy Physics*, vol. 2018, no. 11, 2018. DOI: 10.1007/JHEP11(2018)176.

[14] U. Gran, M. Tornsö, and T. Zingg, "Plasmons in holographic graphene," *SciPost Physics*, vol. 8, no. 6, 2020. DOI: 10.21468/SciPostPhys.8.6.093.

[15] U. Gran, M. Tornsö, and T. Zingg, "Exotic holographic dispersion," *Journal of High Energy Physics*, vol. 2019, no. 2, p. 32, 2019-02. DOI: 10.1007/JHEP02(2019)032.

[16] B. Zwiebach, *A First Course in String Theory*, 2nd ed. Cambridge University press, 2009.

[17] S. A. Hartnoll, A. Lucas, and S. Sachdev. (2018). "Holographic quantum matter." arXiv: 1612.07324 [hep-th].

[18] D. Tong. (2012). "Lectures on String Theory." arXiv: 0908.0333 [hep-th].

[19] M. E. Peskin and D. V. Schroeder, *An Introduction to Quantum Field Theory*. CRC Press, 1995.

[20] J. Erdmenger and M. Ammon, *Gauge/Gravity Duality*. Cambridge University press, 2015.

[21] E. Mauri and H. T. C. Stoof, "Screening of coulomb interactions in holography," *Journal of High Energy Physics*, vol. 2019, no. 4, p. 35, 2019-04. DOI: 10.1007/JHEP04(2019)035.

[22] D. Marolf, W. Kelly, and S. Fischetti, "Conserved Charges in Asymptotically (Locally) AdS Spacetimes," in *Springer Handbook of Spacetime*, A. Ashtekar and V. Petkov, Eds. 2012-11. DOI: 10.1007/978-3-642-41992-8_19.

[23] U. Gran, M. Tornsö, and T. Zingg, "Holographic response of electron clouds," *Journal of High Energy Physics*, vol. 2019, no. 3, p. 19, 2019-03. DOI: 10.1007/JHEP03(2019)019.

[24] S. Maier, *Plasmonics: Fundamentals and Applications*. Springer, 2007.

[25] R. Ruppin, "Surface polaritons of a left-handed medium," *Physics Letters A*, vol. 277, no. 1, pp. 61–64, 2000-11. DOI: 10.1016/S0375-9601(00)00694-0.

[26] V. Giangreco M. Puletti, S. Nowling, L. Thorlacius, and T. Zingg, "Magnetic oscillations in a holographic liquid," *Phys. Rev. D*, vol. 91, no. 8, p. 086 008, 2015. DOI: 10.1103/PhysRevD.91.086008. arXiv: 1501.06459 [hep-th].

[27] M. Ihl, N. Jokela, and T. Zingg, "Holographic anyonization: A systematic approach," *Journal of High Energy Physics*, vol. 2016, no. 6, p. 76, 2016-06. DOI: 10.1007/JHEP06(2016)076.

[28] Wolfram Research, Inc., *Mathematica, Version 12.2*, version 12.1, 2020. [Online]. Available: https://www.wolfram.com/mathematica.

[29] J. M. Martín-García et al., *xAct: Efficient tensor computer algebra for the Wolfram Language*, version 1.1.4, 2020-02. [Online]. Available: http://www.xact.es/.

[30] J. Lebl. (2021-01). "Singular Points and the Method of Frobenius," [Online]. Available: https://math.libretexts.org/@go/page/359.

[31] G. W. Gibbons and S. W. Hawking, "Action integrals and partition functions in quantum gravity," *Phys. Rev. D*, vol. 15, 10 1977. DOI: 10.1103/PhysRevD.15.2752.

[32] R. Emparan, C. V. Johnson, and R. C. Myers, "Surface terms as counterterms in the AdS-CFT correspondence," *Physical Review D*, vol. 60, no. 10, 1999-10. DOI: 10.1103/physrevd.60.104001.

[33] Wolfram Research, Inc., *Wolfram Client library for Python*.

[34] T. Head, M. Kumar, H. Nahrstaedt, G. Louppe, and I. Shcherbatyi, *Scikit-optimize/scikit-optimize*, version v0.8.1, 2020-09. DOI: 10.5281/zenodo.4014775.

[35] T. Zingg, "Thermodynamics of dyonic lifshitz black holes," *Journal of High Energy Physics*, vol. 2011, pp. 1–22, 2011-09. DOI: 10.1007/JHEP09(2011)067.

A. Supplementary Material

A.1 Holographic dictionary

1. The partition functions of the $(d+2)$-dimensional gravitational theory and the dual $(d+1)$-dimensional QFT can be taken to be equal (the GKPW rule).
2. The source h of an operator $\mathcal{O}$ is the boundary value of the dual field.
3. A scalar operator $\mathcal{O}$ is dual to a scalar field ϕ in the bulk.
4. The boundary energy momentum tensor $T^{\mu\nu}$ is dual to the dynamical bulk metric $g_{\mu\nu}$.
5. A boundary conserved current $\mathcal{J}^{\mu}$ is dual to a bulk gauge field A_{μ}.
6. If a source h is dual to a bulk field ϕ, it is canonically identified with the leading behavior of the solution ϕ^* to the bulk equations of motion.
7. The expectation value of the operator sourcing h is canonically identified with the sub-leading behavior of ϕ^*, and is explicitly calculated as $\langle\mathcal{O}\rangle = \frac{\delta S^*}{\delta h}$.
8. The exponent Δ_+ of the sub-leading solution is canonically identified as the scaling dimension of the boundary operator $\mathcal{O}$, and is dependent on the bulk field's mass.
9. A finite temperature T on the boundary equals the Hawking temperature of a black hole in the bulk.
10. The boundary and bulk vector potentials are identified as $\mathcal{A}_{\mu} = \lim_{r\to 0} A_{\mu}$.
11. A finite chemical potently μ on the boundary is the boundary value of the time component of the bulk vector potential.

A.2 Sign conventions

With the Minkowski metric in the mostly plus convention; $\eta_{00} = -1$, $\eta_{ii} = +1$, we define the 4-vector potential and 4-vector current as

$$\begin{aligned} A^\mu = (\phi, A^i), \quad &\implies \quad A_\mu = (-\phi, A_i) \\ J^\mu = (\rho, J^i), \quad &\implies \quad J_\mu = (-\rho, J_i). \end{aligned} \tag{A.1}$$

The electromagnetic field tensor is defined as $F^{\mu\nu} = 2\partial^{[\mu} A^{\nu]}$, from which is follows that

$$F^{\mu\nu} = \begin{bmatrix} 0 & E_x & E_y & E_z \\ -E_x & 0 & B_z & -B_y \\ -E_y & -B_z & 0 & B_x \\ -E_z & B_y & -B_x & 0 \end{bmatrix} \implies F_{\mu\nu} = \begin{bmatrix} 0 & -E_x & -E_y & -E_z \\ E_x & 0 & B_z & -B_y \\ E_y & -B_z & 0 & B_x \\ E_z & B_y & -B_x & 0 \end{bmatrix}. \tag{A.2}$$

Note that with this sign convention, the time components are the ones to change sign. Furthermore, Maxwell's equations reads

$$\partial_\mu F^{\mu\nu} = -J^\nu \quad \text{or} \quad \partial_\nu F^{\mu\nu} = J^\mu \tag{A.3}$$

which gives us explicitly

$$\nabla \cdot \mathbf{E} = \rho \quad \text{and} \quad \nabla \times \mathbf{B} = \mathbf{J} + \frac{\partial \mathbf{E}}{\partial t} \tag{A.4}$$

while the Bianchi identity yields

$$\partial_{[\mu} F_{\nu\rho]} = 0 \quad \implies \quad \nabla \cdot \mathbf{B} = 0 \quad \text{and} \quad \nabla \times \mathbf{E} = -\frac{\partial \mathbf{B}}{\partial t}. \tag{A.5}$$

For the following chapter on differential forms, the sign convention for the Levi-Civita pseudotensor needs to be set. We define it as

$$\varepsilon_{0123} = +1 \quad \implies \quad \varepsilon^{0123} = -1. \tag{A.6}$$

Due to our sign convention of the Minkowksi metric, this is consistent through different number of space dimensions.

A.3 Differential forms

This appendix serves as a quick refresher, or short introduction, to the language of exterior calculus and differential forms which are used throughout this thesis.

A p-form ω is defined as the wedge product of p 1-forms $\mathrm{d}x^i$ as

$$\omega = \frac{1}{p!}\omega_{i_1,\ldots,i_p}\mathrm{d}x^{i_1} \wedge \cdots \wedge \mathrm{d}x^{i_p} \tag{A.7}$$

where we can identify $\omega_{i_1,\ldots,i_p}$ as the corresponding tensor (with covariant index structure!) one might be more accustomed working with. The key takeaway is that we can identify the value of the tensor with indices $i_1 i_2$ as the term (without the factorial compensation for over-counting) in front of $\mathrm{d}x^{i_1} \wedge \mathrm{d}x^{i_2}$, for instance.

The inner product between two 1-forms is the usual;

$$\langle \omega, \eta \rangle = g^{\mu\nu}\omega_\mu \eta_\nu. \tag{A.8}$$

Furthermore, the wedge product is skew-symmetric, i.e $\mathrm{d}x \wedge \mathrm{d}y = -\mathrm{d}y \wedge \mathrm{d}x$, so a wedge product between a p-form ω and a q-form η becomes

$$\omega \wedge \eta = (-1)^{pq}\eta \wedge \omega. \tag{A.9}$$

The volume element of a semi-Riemannian manifold is

$$v = \sqrt{|g|}\mathrm{d}x^1 \wedge \cdots \wedge \mathrm{d}x^n. \tag{A.10}$$

The Hodge star operator is an isomorphism that maps p-forms to $(n-p)$-forms on a manifold M with dimension n;

$$\star : \Omega^p(M) \to \Omega^{(n-p)}(M) \quad \text{such that} \quad \omega \wedge \star\eta = \langle \omega, \eta \rangle v. \tag{A.11}$$

Applying the Hodge star to a p-form yields

$$\star\left(\mathrm{d}x^{i_1} \wedge \cdots \wedge \mathrm{d}x^{i_p}\right) = \frac{\sqrt{|g|}}{(n-p)!} g^{i_1 j_1} \ldots g^{i_p j_p} \varepsilon_{j_1 \ldots j_n} \mathrm{d}x^{j_{p+1}} \wedge \cdots \wedge \mathrm{d}x^{j_n} \tag{A.12}$$

where we use the definition $\varepsilon_{0123\ldots} = +1$. Since the signature of the metric is always -1 for a Lorentzian manifold, we have that

$$\star^2 = (-1)^{p(n-p)+1} \tag{A.13}$$

so that in 4 spacetime dimensions, $\star^2 = -1$ *only on 2-forms*, but in 5 spacetime dimensions, $\star^2 = -1$ *always*! Due to the square, we have an inverse which takes on the sign

$$\star^{-1} = \begin{cases} -\star & n \text{ is odd} \\ (-1)^{p+1}\star & n \text{ is even} \end{cases} \tag{A.14}$$

such that $\star\star^{-1} = 1$. The trick thing to remember when computing the Hodge dual of a form α with our signature convention is:

$$\begin{aligned} &\text{Commute as needed such that } \alpha(\star\alpha) = \mathrm{d}t \wedge \mathrm{d}x \ldots \\ &\text{Add an extra minus sign } \textit{if } \alpha \textit{ contains } \mathrm{d}t \end{aligned} \tag{A.15}$$

Compare this with (A.12); the Levi-Civita tensor ensures the first property; it will give plus for 0123... (i.e. $\mathrm{d}t\wedge\mathrm{d}x\wedge\ldots$) and any permutation that is of equal parity. Furthermore, if α contains $\mathrm{d}t$, the right-hand side will include $g^{00} = -1$. Note that cyclic permutations alternate between being of even/odd parity for an even number of objects.

The exterior derivative takes a p-form to a $p+1$-form, is linear, and specifically,

$$\mathrm{d}(\omega \wedge \eta) = \mathrm{d}\omega \wedge \eta + (-1)^p \omega \wedge \mathrm{d}\eta, \quad \text{for } \omega \in \Omega^p \tag{A.16}$$

where the exterior derivative of a zero-form is the usual derivative. With the compound index I; $\omega = f_I \mathrm{d}x^I = f_1 \mathrm{d}x^1 \wedge f_2 \mathrm{d}x^2 \ldots$, we can write this as

$$\mathrm{d}\omega = \frac{\partial f_I}{\partial x^i} \mathrm{d}x^i \wedge \mathrm{d}x^I. \tag{A.17}$$

With these tools at our disposal, we can write Maxwell's equations quite neatly. We treat the electric and magnetic fields as vectors, so the field tensor decomposes as (compare with (A.2)):

$$F = \mathbf{E} \wedge \mathrm{d}t + \star^{-1}(\mathbf{B} \wedge \mathrm{d}t) \tag{A.18}$$

with $\mathbf{E} = E_x \mathrm{d}x + E_y \mathrm{d}y + E_z \mathrm{d}z$ and so on. The term $E_x \mathrm{d}x \wedge \mathrm{d}t$ means that E_x sits at F_{xt}. Analogously, the term $B_x \mathrm{d}x \wedge \mathrm{d}t$ gets dualized to $+F_{yz}$, since with our sign conventions, $\star(\mathrm{d}x \wedge \mathrm{d}t) = +\mathrm{d}y \wedge \mathrm{d}z$. With the language of differential forms, we can state Stokes generalized theorem;

$$\int_M \mathrm{d}\omega = \oint_{\partial M} \omega \tag{A.19}$$

where we stress the fact that the integral over ∂M is closed - ∂M has no boundary, which is manifest from the identity $\mathrm{d}^2 = 0$, if one were to apply Stokes theorem twice.

With these expressions, Maxwell's equations now reads

$$\mathrm{d}F = 0 \quad \text{and} \quad \mathrm{d} \star F = \star J \tag{A.20}$$

where

$$J = -\rho \mathrm{d}t + \mathbf{J}. \tag{A.21}$$

Compare this with (A.1).

A.4 Homotopy operators

We assume there to be a a homotopy operator $\mathcal{K}$ such that for a form ω;

$$\omega = \mathcal{K}\mathrm{d}\omega + \mathrm{d}\mathcal{K}\omega \quad \text{and} \quad \iota_n \mathcal{K} = 0 \text{ on } \partial M \tag{A.22}$$

Note that $\mathcal{K}$ lowers the degree of the form it acts on. The homotopy operator may be constructed via radial integration, since AdS_5 is naturally foliated into parallel submanifolds (surfaces of constant r) [27].

The variation of the action with $\mathcal{L}[\mathrm{d}A, A]$ is

$$\delta S = \int_M \delta A \wedge \frac{\partial \mathcal{L}}{\partial A} + \int_M \delta(\mathrm{d}A) \wedge \frac{\partial \mathcal{L}}{\partial \mathrm{d}A} \tag{A.23}$$

The first term we will leave as is. The second term splits into two, using the homotopy operator;

$$\int_M \delta(\mathrm{d}A) \wedge \frac{\partial \mathcal{L}}{\partial \mathrm{d}A} = \int_M \delta(\mathrm{d}A) \wedge \mathcal{K}\mathrm{d}\left(\frac{\partial \mathcal{L}}{\partial \mathrm{d}A}\right) + \int_M \delta(\mathrm{d}A) \wedge \mathrm{d}\mathcal{K}\frac{\partial \mathcal{L}}{\partial \mathrm{d}A} \tag{A.24}$$

The second term can be written as a total derivative, since $\mathrm{d}^2 = 0$;

$$\begin{aligned} \int_M \delta(\mathrm{d}A) \wedge \mathrm{d}\mathcal{K}\frac{\partial \mathcal{L}}{\partial \mathrm{d}A} &= \int_M \mathrm{d}\left(\delta(\mathrm{d}A) \wedge \mathcal{K}\frac{\partial \mathcal{L}}{\partial \mathrm{d}A}\right) + 0 \\ &= \oint_{\partial M} \delta(\mathrm{d}A) \wedge \mathcal{K}\frac{\partial \mathcal{L}}{\partial \mathrm{d}A} \implies \oint_{\partial M} \delta\mathcal{B} \wedge \star\mathcal{M} \end{aligned} \tag{A.25}$$

by Stokes' theorem. Hence we identify

$$\begin{aligned} \mathcal{M} = \mathcal{K}\frac{\partial \mathcal{L}}{\partial \mathrm{d}A} = \int^r \mathrm{d}r * F \implies \\ \mathcal{M}_y = \left\langle \int_{r_h}^r *F,\, \mathrm{d}y \wedge \mathrm{d}t \right\rangle \end{aligned} \tag{A.26}$$

as $\delta \mathrm{d}A$ must be in the transverse direction, and we want the magnetization in the y-direction.

B. Calculations

B.1 Gauge solutions

We start with the radial component of the metric;

$$\begin{aligned} 0 = \delta_\xi g_{rr} &= \xi^r \partial_r g_{rr} + 2 g_{rr} \partial_r \xi^r \\ &\propto \zeta'^r + \left(\frac{g'}{g^2} - \frac{1}{r} \right) \zeta^r \propto \frac{\mathrm{d}}{\mathrm{d}r} \left[\exp\left\{ \int^r \mathrm{d}\mathfrak{r} \left(\frac{g'(\mathfrak{r})}{g^2(\mathfrak{r})} - \frac{1}{\mathfrak{r}} \right) \right\} \zeta^r \right] \\ &\implies \zeta^r = c_1 \frac{r}{\sqrt{g}} = c_1 r \sqrt{f}. \end{aligned} \tag{B.1}$$

For the components of the form $g_{\mu r}$ with $\mu = t, x, y, z$ we can use the fact that the metric is diagonal;

$$\delta_\xi g_{\mu r} = g_{\mu\mu} \partial_r \xi^\mu + g_{rr} \partial_\mu \xi^r. \tag{B.2}$$

The calculations are then straight-forward;

$$\begin{aligned} \mu = t: \quad & 0 = g_{tt} \partial_r \xi^t + g_{rr} \partial_t \xi^r \\ & \propto f \zeta'^t + \mathrm{i}\omega g \zeta^r \implies \zeta'^t = \frac{-\mathrm{i}\omega c_1 r}{f^{3/2}} \\ & \implies \zeta^t = -\mathrm{i}\omega c_1 \int^r \mathrm{d}\mathfrak{r} \, \frac{\mathfrak{r}}{f^{3/2}(\mathfrak{r})} + c_2 \\ \mu = x: \quad & 0 = g_{xx} \partial_r \xi^x + g_{rr} \partial_x \xi^r \\ & \propto \zeta'^x + \mathrm{i}k g \zeta^r \implies \zeta'^x = \frac{-\mathrm{i}k c_1 r}{\sqrt{f}} \\ & \implies \zeta^x = -\mathrm{i}k c_1 \int^r \mathrm{d}\mathfrak{r} \, \frac{\mathfrak{r}}{\sqrt{f(\mathfrak{r})}} + c_3 \\ \mu = y: \quad & 0 = \partial_r \xi^y = 0 \\ & \implies \zeta^y = c_4 \\ \mu = z: \quad & 0 = g_{zz} \partial_r \xi^z + g_{rr} \partial_z \xi^r \\ & \propto \zeta'^z + \lambda_2 g \zeta^r \implies \zeta'^z = \frac{-\lambda_2 c_1 r}{\sqrt{f}} \\ & \implies \zeta^z = -\lambda_2 c_1 \int^r \mathrm{d}\mathfrak{r} \, \frac{\mathfrak{r}}{\sqrt{f(\mathfrak{r})}} + c_5. \end{aligned} \tag{B.3}$$

Finally for the gauge field, we only have a non-zero time component, so

$$\begin{aligned} 0 = \delta_\xi A_r + \partial_r \Lambda = h(r) \partial_r \xi^t + \partial_r \Lambda = \frac{-\mathrm{i}\omega c_1 h r}{f^{3/2}} + L\theta' \\ \implies \theta = \mathrm{i}\omega c_1 \int^r \mathrm{d}\mathfrak{r} \, \frac{\mathfrak{r}\, h(\mathfrak{r})}{f^{3/2}(\mathfrak{r})} + c_6 \end{aligned} \tag{B.4}$$

meaning that the six gauge parameters are determined up to the six integration constants $c_1, \ldots, c_6$. These can be used to compute the pure gauge solutions to the modes. The diagonal solutions are

$$\begin{aligned}
\delta_\xi g_{tt} &= \xi^r \partial_r g_{tt} + 2\frac{L^2 f}{r^2}\mathrm{i}\omega\xi^t \\
&= \xi^r L^2 \left(\frac{2f - rf'}{r^3}\right) + \frac{2\mathrm{i}\omega L^2 f}{r^2}\xi^t \\
&= \frac{L^2}{r^2}\left[c_1\left(\sqrt{f}(2f - rf') + 2\omega^2 f\int^r \mathrm{d}\mathfrak{r}\,\frac{\mathfrak{r}}{f^{3/2}(\mathfrak{r})}\right) + 2c_2\mathrm{i}\omega f\right]\mathrm{e}^{-\mathrm{i}\omega t + \mathrm{i}kx + \lambda_2 z} \\
\delta_\xi g_{xx} &= \xi^r \partial_r g_{xx} + 2\frac{L^2}{r^2}\mathrm{i}k\xi^x \\
&= \frac{2L^2}{r^2}\left[c_1\left(-\sqrt{f} + k^2\int^r \mathrm{d}\mathfrak{r}\,\frac{\mathfrak{r}}{\sqrt{f(\mathfrak{r})}}\right) + c_3\mathrm{i}k\right]\mathrm{e}^{-\mathrm{i}\omega t + \mathrm{i}kx + \lambda_2 z} \\
\delta_\xi g_{yy} &= \xi^r \partial_r g_{yy} = -c_1\frac{2L^2}{r^2}\sqrt{f}\mathrm{e}^{-\mathrm{i}\omega t + \mathrm{i}kx + \lambda_2 z} \\
\delta_\xi g_{zz} &= \xi^r \partial_r g + 2\frac{L^2}{r^2} z z \lambda_2 \xi^z \\
&= \frac{-2L^2}{r^2}\left[c_1\left(\sqrt{f} + \lambda^2\int^r \mathrm{d}\mathfrak{r}\,\frac{\mathfrak{r}}{\sqrt{f(\mathfrak{r})}}\right) + c_5\lambda_2\right]\mathrm{e}^{-\mathrm{i}\omega t + \mathrm{i}kx + \lambda_2 z}.
\end{aligned} \tag{B.5}$$

Recall that $\delta_\xi g_{\mu r} = 0$ for all values of μ by construction. The off-diagonal solutions are slightly more intricate;

$$\begin{aligned}
\delta_\xi g_{tx} &= g_{tt}\partial_x \xi^t + g_{xx}\partial_t \xi^x \\
&= -\frac{L^2}{r^2}\left[c_1\omega k\left(f\int^r \mathrm{d}\mathfrak{r}\,\frac{\mathfrak{r}}{f^{3/2}(\mathfrak{r})} + \int^r \mathrm{d}\mathfrak{r}\,\frac{\mathfrak{r}}{\sqrt{f(\mathfrak{r})}}\right) + c_2\mathrm{i}\omega f + c_3\mathrm{i}\omega\right]\mathrm{e}^{-\mathrm{i}\omega t + \mathrm{i}kx + \lambda_2 z} \\
\delta_\xi g_{ty} &= g_{yy}\partial_t \xi^y = -c_4\frac{L^2}{r^2}\mathrm{i}\omega\mathrm{e}^{-\mathrm{i}\omega t + \mathrm{i}kx + \lambda_2 z} \\
\delta_\xi g_{tz} &= g_{tt}\partial_z \xi^t + g_{zz}\partial_t \xi^z \\
&= \frac{L^2}{r^2}\left[c_1\lambda_2\mathrm{i}\omega\left(f\int^r \mathrm{d}\mathfrak{r}\,\frac{\mathfrak{r}}{f^{3/2}(\mathfrak{r})} + \int^r \mathrm{d}\mathfrak{r}\,\frac{\mathfrak{r}}{\sqrt{f(\mathfrak{r})}}\right) - c_2\lambda_2 f - c_5\mathrm{i}\omega\right]\mathrm{e}^{-\mathrm{i}\omega t + \mathrm{i}kx + \lambda_2 z} \\
\delta_\xi g_{xy} &= g_{yy}\partial_x \xi^y = c_4\frac{L^2}{r^2}\mathrm{i}k\mathrm{e}^{-\mathrm{i}\omega t + \mathrm{i}kx + \lambda_2 z} \\
\delta_\xi g_{xz} &= g_{zz}\partial_z \xi^z + g_{zz}\partial_x \xi^z \\
&= -\frac{L^2}{r^2}\left[2c_1\lambda_2\mathrm{i}k\int^r \mathrm{d}\mathfrak{r}\,\frac{\mathfrak{r}}{\sqrt{f(\mathfrak{r})}} - c_2\lambda_2 - c_5\mathrm{i}k\right]\mathrm{e}^{-\mathrm{i}\omega t + \mathrm{i}kx + \lambda_2 z} \\
\delta_\xi g_{yz} &= g_{yy}\partial_z \xi^y = c_4\frac{L^2}{r^2}\lambda_2\mathrm{e}^{-\mathrm{i}\omega t + \mathrm{i}kx + \lambda_2 z}.
\end{aligned} \tag{B.6}$$

Continuing with the gauge field;

$$\begin{aligned}
\delta A_t &= \xi^r \partial_r A_t + A_t \partial_t \xi^t + \partial_t \Lambda \\
&= \left[c_1 \left(r\sqrt{f} h' - \omega^2 h \int^r \mathrm{d}\mathfrak{r} \, \frac{\mathfrak{r}}{f^{3/2}(\mathfrak{r})} + \omega^2 \int^r \mathrm{d}\mathfrak{r} \, \frac{\mathfrak{r}\, h(\mathfrak{r})}{f^{3/2}(\mathfrak{r})} \right) - \mathrm{i}\omega(hc_2 + c_6) \right] \mathrm{e}^{-\mathrm{i}\omega t + \mathrm{i}kx + \lambda_2 z} \\
\delta A_x &= A_t \partial_x \xi^t + \partial_x \Lambda \\
&= \left[c_1 k\omega \left(h \int^r \mathrm{d}\mathfrak{r} \, \frac{\mathfrak{r}}{f^{3/2}(\mathfrak{r})} - \int^r \mathrm{d}\mathfrak{r} \, \frac{\mathfrak{r}\, h(\mathfrak{r})}{f^{3/2}(\mathfrak{r})} \right) + \mathrm{i}k(hc_2 + c_6) \right] \mathrm{e}^{-\mathrm{i}\omega t + \mathrm{i}kx + \lambda_2 z} \\
\delta A_y &= 0 \\
\delta A_z &= A_t \partial_z \xi^t + \partial_z \Lambda \\
&= \left[c_1 \mathrm{i}\omega\lambda_2 \left(-h \int^r \mathrm{d}\mathfrak{r} \, \frac{\mathfrak{r}}{f^{3/2}(\mathfrak{r})} + \int^r \mathrm{d}\mathfrak{r} \, \frac{\mathfrak{r}\, h(\mathfrak{r})}{f^{3/2}(\mathfrak{r})} \right) + \lambda_2(hc_2 + c_6) \right] \mathrm{e}^{-\mathrm{i}\omega t + \mathrm{i}kx + \lambda_2 z}.
\end{aligned} \tag{B.7}$$

These are our sought after gauge solutions! As these are gauge fields, a constant shift doesn't matter, which is why we can perform the integrals from anywhere in the region $(0, 1)$ to r. We're mainly interested in their behavior near the boundary, so we choose 0 for simplicity. Some of these integrals can not be solved analytically, and are solved for by expanding the integrand in a power series. To get linearly independent solutions, one simply sets one of the integration constants to unity and the others to zero.

B.2 Counterterms

Performing variation of the Einstein-Hilbert action gives

$$\delta S = \int_M \mathrm{d}^{d+2}x\,\sqrt{-g}\,\left(R_{\mu\nu} - \frac{1}{2}g_{\mu\nu}R\right)\delta g^{\mu\nu} + \int_M \mathrm{d}^{d+2}x\,\sqrt{-g}\,g^{\mu\nu}\delta R_{\mu\nu}. \tag{B.8}$$

The Palatini identity tells us that

$$\delta R_{\mu\nu} = \nabla_\rho \delta\Gamma^\rho_{\mu\nu} - \nabla_\nu \delta\Gamma^\rho_{\mu\rho} \implies g^{\mu\nu}\delta R_{\mu\nu} = \nabla_\mu g^{\mu\nu} g^{\rho\sigma}\left(\delta\partial_\rho g_{\nu\sigma} - \delta\partial_\nu g_{\rho\sigma}\right) \equiv \nabla_\mu H^\mu \tag{B.9}$$

where we have used that $\delta g_{\mu\nu} = \delta g^{\mu\nu} = 0$ when computing the variation of the affine connection. Using the fact that the metric is covariantly constant, in combination with Stokes' theorem on second term in (B.8), we obtain

$$\int_M \mathrm{d}^{d+2}x\,\nabla_\mu\left[\sqrt{-g}\,H^\mu\right] = \oint_{\partial M} \mathrm{d}^{d+1}x\,\sqrt{-\gamma}\,n_\mu H^\mu. \tag{B.10}$$

With the definition of the induced metric, we can write

$$\begin{aligned} n_\mu H^\mu &= n_\mu g^{\mu\nu} g^{\rho\sigma}\left(\delta\partial_\rho g_{\nu\sigma} - \delta\partial_\nu g_{\rho\sigma}\right) \\ &= 2n^\mu\left(\gamma^{\rho\sigma} + \cancel{s n^\rho n^\sigma}\right)\delta\partial_{(\rho}g_{\mu)\sigma} \\ &= -\gamma^{\rho\sigma} n^\mu \delta\partial_\mu g_{\rho\sigma} \end{aligned} \tag{B.11}$$

where we have used the fact that vanishing metric on the boundary implies vanishing tangential derivatives of the metric; $\gamma^{\rho\sigma}\delta\partial_\rho g_{\mu\sigma} = 0$. Nevertheless, since derivatives of the metric in general are not required to vanish, the variation of the action may not be well-defined. Adding the Gibbon-Hawking-York counterterm to the action, will yield an additional contribution from the variation of (the trace of) the extrinsic curvature K as

$$\begin{aligned} \delta K = \gamma^{\mu\nu}\delta\nabla_\mu n_\nu &= \gamma^{\mu\nu}\left(\cancel{\delta(\partial_\mu n_\nu)} - \delta\Gamma^\rho_{\mu\nu} n_\rho\right) \\ &= -\frac{1}{2}\gamma^{\mu\nu} n^\sigma\left(\cancel{\delta\partial_\mu g_{\mu\sigma}} + \cancel{\delta\partial_\nu g_{\nu\sigma}} - \delta\partial_\sigma g_{\mu\nu}\right) \\ &= \frac{1}{2}\gamma^{\mu\nu} n^\sigma \delta\partial_\sigma g_{\mu\nu} \end{aligned} \tag{B.12}$$

again requiring vanishing tangential derivatives of the metric. This term is with relabeling of indices equal to the one in (B.11) up to a constant factor, and the effect of the counterterm should now be clear.

DEPARTMENT OF PHYSICS
CHALMERS UNIVERSITY OF TECHNOLOGY
Gothenburg, Sweden
www.chalmers.se

CHALMERS
UNIVERSITY OF TECHNOLOGY